Prior SARS-CoV-2 infection enhances and reshapes spike protein-specific memory induced by vaccination

Véronique Barateau, Loïc Peyrot, Carla Saade, Bruno Pozzetto, Karen Brengel-Pesce, Mad-Hélénie Elsensohn, Omran Allatif, Nicolas Guibert, Christelle Compagnon, Natacha Mariano, et al.

CORONAVIRUS

Prior SARS-CoV-2 infection enhances and reshapes spike protein–specific memory induced by vaccination

Véronique Barateau[1]†, Loïc Peyrot[1]†, Carla Saade[1]†, Bruno Pozzetto[1,2]†, Karen Brengel-Pesce[3]†, Mad-Hélénie Elsensohn[4,5], Omran Allatif[1], Nicolas Guibert[6], Christelle Compagnon[3], Natacha Mariano[7], Julie Chaix[7], Sophia Djebali[1], Jean-Baptiste Fassier[6], Bruno Lina[1,8], Katia Lefsihane[1], Maxime Espi[1], Olivier Thaunat[1], Jacqueline Marvel[1], Manuel Rosa-Calatrava[1], Andres Pizzorno[1], Delphine Maucort-Boulch[4,5], Laetitia Henaff[1,9], Mitra Saadatian-Elahi[1,9], Philippe Vanhems[1,9], Stéphane Paul[1,2]*‡, Thierry Walzer[1]*‡, Sophie Trouillet-Assant[1,3]*‡, Thierry Defrance[1]*‡

The diversity of vaccination modalities and infection history are both variables that have an impact on the immune memory of individuals vaccinated against SARS-CoV-2. To gain more accurate knowledge of how these parameters imprint on immune memory, we conducted a long-term follow-up of SARS-CoV-2 spike protein–specific immune memory in unvaccinated and vaccinated COVID-19 convalescent individuals as well as in infection-naïve vaccinated individuals. Here, we report that individuals from the convalescent vaccinated (hybrid immunity) group have the highest concentrations of spike protein–specific antibodies at 6 months after vaccination. As compared with infection-naïve vaccinated individuals, they also display increased frequencies of an atypical mucosa-targeted memory B cell subset. These individuals also exhibited enhanced T_H1 polarization of their SARS-CoV-2 spike protein–specific follicular T helper cell pool. Together, our data suggest that prior SARS-CoV-2 infection increases the titers of SARS-CoV-2 spike protein–specific antibody responses elicited by subsequent vaccination and induces modifications in the composition of the spike protein–specific memory B cell pool that are compatible with enhanced functional protection at mucosal sites.

INTRODUCTION

Since the emergence of severe acute respiratory syndrome coronavirus 2 (SARS-CoV-2), many factors have altered individual susceptibility to infection. Coronavirus disease 2019 (COVID-19)–convalescent individuals are generally less likely to be infected a second time, and they often develop less severe symptoms upon reinfection (*1*, *2*). Adenovirus-based or mRNA vaccines have shown remarkable efficacy in protecting against infections by SARS-CoV-2, reducing the risk of severe illness, hospitalization, and death (*3*, *4*). Introduction of diverse COVID-19 vaccines and vaccination regimens administered to infection-naïve individuals or individuals with previous SARS-CoV-2 infection has created a variety of immune imprints that need to be compared to prioritize worse-off populations for additional booster doses of vaccine. For example, convalescent individuals develop much higher titers of binding and neutralizing spike protein–specific antibodies (Abs) after mRNA vaccine (*5*, *6*) or adenoviral-based vaccine (*7*, *8*) than naïve individuals. This so-called "hybrid" immunity is associated with stronger memory B and T cell antiviral responses (*9*) with better neutralizing Abs (*10*) and with a lower risk of SARS-CoV-2 reinfection (*11*–*14*).

Despite extensive COVID-19 vaccine coverage, at least in Western countries, breakthrough infections in fully immunized individuals continue to increase worldwide (*15*). This is partly because of the emergence of SARS-CoV-2 variants of concern (VOCs), such as Omicron subvariants, which are poorly neutralized by vaccine-elicited Abs (*16*), and partly because of the waning of the serum Ab barrier over time. We and others have shown that the Ab titers induced by infection (*17*, *18*) or vaccination (*19*, *20*) gradually decline, which correlates with the risk of reinfection (*21*, *22*). Many individuals have very low concentrations of spike protein–specific Abs 6 months after vaccination (*20*), which are probably ineffective in protecting against infection and transmission (*23*, *24*). This has led health authorities to recommend a third vaccine dose (*25*) to boost immunity and confer better protection against infection or reinfection (*26*). However, besides its serological component (serum Abs), immune memory also includes a cellular component (memory lymphocytes) able to generate a swift and amplified immune response if the serological memory barrier fails to control reinfection. Moreover, the frequencies of SARS-CoV-2 spike protein–specific memory T and B lymphocytes elicited by infection or vaccination are more stable over time than the serum

[1]CIRI-Centre International de Recherche en Infectiologie, Univ Lyon, Université Claude Bernard Lyon 1 Inserm, U1111, CNRS, UMR5308, ENS Lyon, Université Jean Monnet de Saint-Etienne, Lyon 69007, France. [2]Immunology laboratory, CIC1408, CHU Saint Etienne, Saint Etienne 42055, France. [3]Laboratoire Commun de Recherche Hospices Civils de Lyon-bioMérieux, Hospices Civils de Lyon, Hopital Lyon Sud, Pierre-Bénite 69495, France. [4]Hospices Civils de Lyon, Pôle Santé Publique, Service de Biostatistique et Bioinformatique, Lyon 69003, France. [5]CNRS, UMR 5558, Laboratoire de Biométrie et Biologie Évolutive, Équipe Biostatistique-Santé, Villeurbanne 69100, France. [6]Occupational Health and Medicine Department, Hospices Civils de Lyon, Université Claude Bernard Lyon1, Ifsttar, UMRESTTE, UMR T_9405, Lyon University, Avenue Rockefeller, Lyon 69008, France. [7]BIOASTER, 40 Avenue Tony Garnier, Lyon 69007, France. [8]Virology laboratory, Institute of Infectious Agents, National Reference Centre for Respiratory Viruses, Hospices Civils de Lyon, Lyon 69317, France. [9]Service D'Hygiène, Épidémiologie, Infectiovigilance et Prévention, Hôpital Édouard Herriot, Hospices Civils de Lyon, Lyon 69008, France.
*Corresponding author. Email: thierry.defrance@inserm.fr (T.D.); stephane.paul@chu-st-etienne.fr (S.P.); sophie.trouillet-assant@chu-lyon.fr (S.T.-A.); thierry.walzer@inserm.fr (T.W.)
†These authors contributed equally to this work.
‡Co-senior authors.

titers of neutralizing Abs (*9*, *17*, *27*). Despite this, the titers of neutralizing Abs are frequently considered to be the only correlate of vaccine efficacy, and the contribution of cellular memory is often overlooked.

With regard to all these considerations, we compared serological and cellular immune memory in unvaccinated or vaccinated individuals with past history of SARS-CoV-2 infection and in infection-naïve vaccinated individuals. Here, we show that hybrid immunity (defined as previous infection and vaccination) is superior to other forms of immunity induced by infection or vaccination only, in terms of spike protein–specific Ab concentrations and serum neutralizing potential. Our data also show that cellular spike protein–specific B cell memory (mBC) is less susceptible to quantitative variations than its serological counterpart but is more subject to qualitative changes instructed by the infection history of the host. In particular, we report that individuals from the hybrid immunity group, as compared with infection-naïve vaccinated individuals, display increased frequencies of an atypical [immunoglobulin D $(IgD)^{-}CD27^{-}$] mucosa-targeted mBC subset also designated as DN2 (for double-negative type 2) mBCs. They are also characterized by enhanced T helper cell 1 (T_H1) polarization of their SARS-CoV-2 spike protein–specific follicular T helper (T_{FH}) cell pool. Together, our data strongly suggest that vaccination of previously infected individuals reinforces the serological component of mBC and reshapes the composition and trafficking pattern of the mBC compartment.

RESULTS

Clinical characteristics of study population

This study was conducted on 613 individuals from different cohorts [Immunonosocor (*28*) or Covid-Ser (*29*)] subdivided into (i) convalescent patients after severe or mild COVID-19, (ii) vaccinated convalescent patients (having all experienced a mild form of COVID-19) who received either one or two doses of the Pfizer BNT162b2 mRNA vaccine or one dose of the adenoviral-based vaccine ChAdOx1, and (iii) COVID-19–naïve individuals fully vaccinated with two doses of BNT162b2 or one dose of ChAdOx1 followed by one dose of BNT162b2. For the sake of simplicity, the ChAdOx1 and BNT162b2 vaccines will be hereafter referred to as ChAdOx and BNT, respectively. All infections occurred during the first wave of the pandemic (mainly due to 20A lineage). Together, these different clinical situations define seven groups of individuals (Table 1), in whom we monitored B and T cell immunity against the SARS-CoV-2 spike protein or its receptor binding domain (RBD) at 6 months after either infection or vaccination. The different humoral and cellular immunity parameters that were monitored in participants of these cohorts are summarized in fig. S1.

It is important to note some clinical differences between the seven groups of individuals. First, the group of convalescent patients who experienced severe COVID-19 had a smaller proportion of females (39.34%) and were older (median age of 67 years) in comparison with the other groups of individuals, for whom the proportion of females ranged from 68.57 to 90%, and the median age ranged from 32 to 49 years old (Table 1). Second, these individuals had a higher prevalence of comorbidities (79.78%) in comparison with other groups of individuals, for whom the prevalence of comorbidities ranged from 5.71 to 41.17% (Table 1). The demographic data for our cohort of patients with severe COVID-19 are in line with what was previously described in the literature (*30*, *31*). As for the delay between last immunization and blood sampling, it was about 6 months (180 days) for all groups except for the severe COVID-19 group, for which the delay was of 9 months (289 days) (Table 1). No major difference was observed regarding the demographic data between unvaccinated convalescent patients with mild COVID-19, convalescent vaccinated, and naïve vaccinated individuals. Last, for a more accurate estimation of the rate of infection events for convalescent vaccinated and naïve vaccinated individuals, an intermediate blood sample was collected between vaccination and the 6 months' time point. We monitored the occurrence of breakthrough infections in our cohorts by assessing RBD IgG titers using the bioMerieux Vidas SARS-CoV-2 IgG assay. In our hands, this assay was more reliable than monitoring seroconversion against the N antigen. A breakthrough infection was identified by a rebound of RBD Ab titers instead of the steady decline that normally occurs in the absence of viral exposure. This follow-up of the RBD Ab titers revealed that none of the participants became infected/reinfected in the 6 months between vaccination/infection and blood sampling.

SARS-CoV-2 spike protein–specific serological mBC is superior in convalescent vaccinated individuals

Despite the broad knowledge of infection-acquired and vaccine-induced immunity, studies comparing the virus-specific immune parameters between convalescent, convalescent vaccinated (with different vaccines), and infection-naïve vaccinated individuals at late time points after infection or vaccination are still sparse. We first examined the parameters of serological mBC: the titers, avidity, and neutralization potential of anti-S1 and anti-RBD serum Abs. Concentrations of serum RBD-specific IgG were by far the highest among convalescent vaccinated patients (hybrid immunity) regardless of the vaccination regimen (Fig. 1A and fig. S2A). The median [interquartile range (IQR)] values expressed in binding Ab unit (BAU) per milliliter in convalescent vaccinated individuals were 1214 (760.9 to 2758) for BNT one dose, 1193 (860.5 to 2448) for BNT two doses, and 851 (330.6 to 1252) for ChAdOx one dose. Unvaccinated convalescent individuals had the lowest RBD-specific IgG concentrations, especially if their COVID-19 course was mildly symptomatic [median (IQR): 80.51 (33.34 to 161.2) and 206.3 (114.1 to 342.2) for mild and severe patients, respectively], whereas vaccinated individuals without prior infection (vaccine-induced immunity) showed intermediate Ab concentrations irrespective of the vaccination regimen [median (IQR): 180 (121.3 to 292.4) for the BNT two doses and 249 (174 to 369.2) for the ChAdOx/BNT combination]. The differences in RBD-specific IgG concentrations between groups persisted after adjustment for age, sex, and the delay between vaccination or infection and blood sampling (Fig. 1B). The serum spike protein–specific IgA Ab concentrations measured in subgroups of individuals followed the same trend as anti-RBD IgG concentrations, with the highest concentrations found in convalescent vaccinated individuals (Fig. 2A and fig. S2B). The ability of serum samples to prevent Vero E6 cell infection by SARS-CoV-2 isolates belonging to the 19A (B38 lineage), the Delta (B.1.617.2 lineage), or the Omicron (B.1.1.529) clade was then assessed with a 50% plaque reduction neutralization test ($PRNT_{50}$) assay (*32*). Serum samples from convalescent vaccinated individuals exhibited 5- to 10-fold higher serum neutralizing Ab titers against the 19A or Delta variants

Table 1. Clinical characteristics of individuals analyzed in this study. NA, not applicable; IQR, interquartile range.

	Unvaccinated convalescent participants		Convalescent vaccinated participants			COVID-19–naïve vaccinated participants	
	Mild COVID-19	Severe COVID-19	BNT162b2	BNT162b2-BNT162b2	ChAdOx1	BNT162b2-BNT162b2	ChAdOx1-BNT161b2
n	203	183	34	50	32	76	35
Demographic data							
Female, *n* (%)	168 (82.75)	72 (39.34)	29 (85.29)	45 (90)	23 (71.87)	57 (75)	24 (68.57)
Age at blood sampling (years), median (IQR)	40 (31–49)	67 (56–75)	42 (35–52)	49 (32–54)	35.5 (30–42.5)	48 (39–56)	32 (28–40)
Anti-RBD IgG concentrations (BAU/ml), median (IQR)	80.51 (33.34–161.2)	206.3 (114.1–342.2)	1214 (760.9–2758)	1193 (860.5–2448)	851.8 (330.6–1252)	180 (121.3–292.4)	249 (174–369.2)
Body mass index,* *n*	203	148	34	50	32	74	34
Body mass index, median (IQR)	23.80 (21.22–26.72)	26.96 (24.45–30.37)	23.61 (21.14–26.33)	24.67 (20.09–27.73)	23.23 (21.13–25.86)	24.34 (21.78–30.02)	22.29 (20.48–24.03)
Currently smoker, * *n* (%)	20/202 (9.9)	4/152 (2.63)	8/34 (23.52)	4/49 (8.16)	1/30 (3.33)	20/54 (37.03)	8/18 (44.44)
Alcohol consumption * (daily), *n* (%)	1/203 (0.49)	6/108 (5.55)	0/34 (0)	3/50 (6)	0/30 (0)	2/54 (3.70)	0/17 (0)
Comorbidities							
Presence of comorbidity, * *n* (%)	72/202 (35.64)	146/183 (79.78)	14/34 (41.17)	19/50 (38)	8/32 (25)	25/76 (32.89)	2/35 (5.71)
Neurological disorders,* *n* (%)	3 (1.48)	8 (4.37)	2 (5.88)	2 (4)	0 (0)	1 (1.31)	0 (0)
Cardiovascular disorders, * *n* (%)	4 (1.98)	82 (44.80)	1 (2.94)	3 (6)	1 (3.12)	0 (0)	0 (0)
Hypertension,* *n* (%)	11 (5.44)	65 (35.51)	2 (5.88)	8 (16)	0 (0)	4 (5.26)	0 (0)
Heart failure,* *n* (%)	1 (0.49)	24 (13.11)	0 (0)	0 (0)	0 (0)	0 (0)	0 (0)
Diabetes,* *n* (%)	6 (2.97)	34 (18.57)	0 (0)	2 (4)	0 (0)	4 (5.26)	0 (0)
Immune deficiency, * *n* (%)	1 (0.49)	9 (4.91)	0 (0)	0 (0)	0 (0)	0 (0)	0 (0)
Liver disease,* *n* (%)	0 (0)	15 (8.19)	0 (0)	1 (2)	0 (0)	1 (1.31)	0 (0)
Kidney disease, * *n* (%)	2 (0.99)	18 (9.83)	0 (0)	0 (0)	2 (6.25)	1 (1.31)	0 (0)
Cancer,* *n* (%)	4 (1.98)	19 (10.38)	1 (2.94)	0 (0)	1 (3.12)	2 (2.63)	0 (0)
Hypothyroidy,* *n* (%)	12 (5.94)	17 (9.28)	3 (8.82)	2 (4)	0 (0)	6 (7.89)	1 (2.85)
Rheumatic disease, **n* (%)	5 (2.47)	20 (10.92)	2 (5.88)	2 (4)	1 (3.12)	1 (1.31)	1 (2.85)
Chronic lung disease,* *n* (%)	12 (5.94)	12 (6.55)	4 (11.76)	2 (4)	3 (9.37)	6 (7.89)	1 (2.85)
Other comorbidities, *n* (%)	44 (21.78)	99 (54.09)	4 (11.76)	5 (10)	4 (12.5)	6 (7.89)	0
Infection/vaccination information							
Delay infection—vaccination (days), median (IQR)	NA	NA	335 (288.8–361.5)	292 (281.3–301.8)	324.5 (311.8–333)	NA	NA
Delay infection—blood sample (days), median (IQR)	186 (180–196)	289 (267–308)	NA	NA	NA	NA	NA
Delay vaccination—blood sample (days), median (IQR)	NA	NA	194 (177–226)	223 (211–238)	214 (196–229)	190 (178–194)	183 (175–188)

*Missing data.

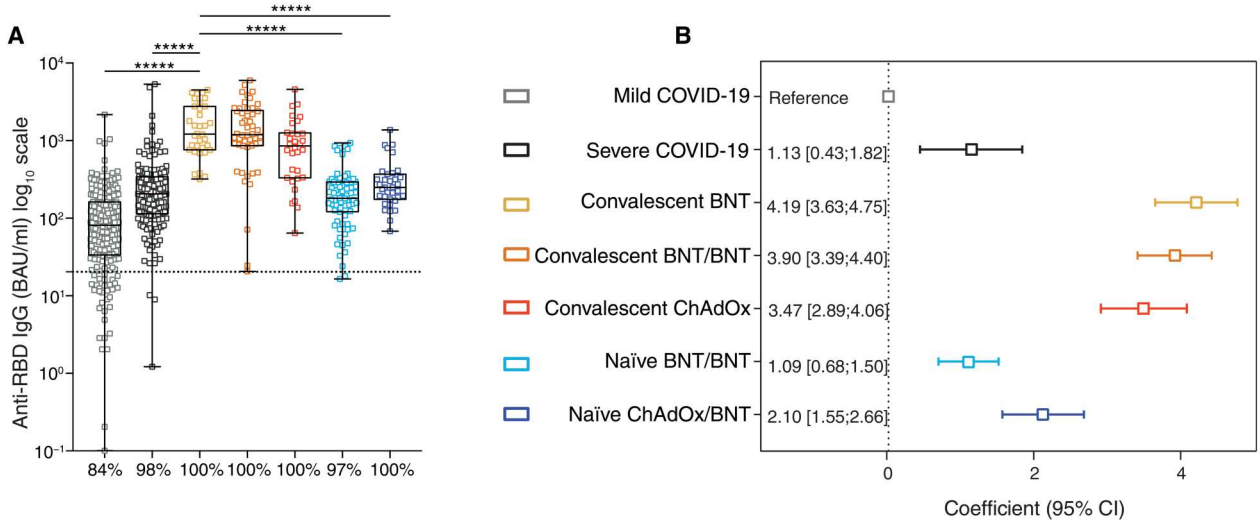

Fig. 1. Convalescent vaccinated individuals have very high titers of SARS-CoV-2 RBD-specific IgG. (**A**) Serum samples from unvaccinated convalescent individuals after mild ($n = 203$) or severe COVID-19 ($n = 183$), convalescent individuals vaccinated with one (BNT, $n = 34$) or two (BNT/BNT, $n = 50$) doses of the BNT vaccine or one dose of the ChAdOx vaccine ($n = 32$), or naïve individuals vaccinated with the BNT/BNT ($n = 76$) or ChAdOx/BNT combination ($n = 35$) were assayed for RBD-specific IgG concentrations 6 months after vaccination or infection. Concentrations are expressed in BAU/ml. Each serum sample was evaluated as a single measurement. The dotted line indicates the positive detection threshold according to the manufacturer. A $\log_{10}$ scale was used for the representation of the data. The percentages of samples above the positive threshold are indicated below the graph. Data are expressed as box-and-whiskers plots showing median (horizontal line inside the box), IQR (upper and lower horizontal lines of the box), and minimum and maximum (whiskers), and each dot corresponds to one individual. For the sake of clarity, statistical significance values derived from the adjusted model are indicated for a limited number of comparisons. A complete matrix of statistical significance values is shown in fig. S2A. (**B**) Forest plot depicting the additional concentration of RBD-specific IgG ($\log_2$-transformed) in the different groups relative to the mild convalescent reference group after adjustment for age, sex, and delay between infection or vaccination and IgG measurement. The squares represent the regression coefficients, and bars indicate the 95% confidence interval (CI). For example, a coefficient of 4.19 for the convalescent BNT group means that, on average, the quantity of specific IgGs against RBD is 18-fold ($2^{4.19}$) higher than in the reference group (mild COVID-19) after adjustment for covariates. *****$P < 0.00001$.

than those from individuals from the convalescent or naïve vaccinated groups (Fig. 2, B and C, and fig. S2, C to E). As for the Omicron variant, we observed a marked decrease in neutralizing Ab titers that ranged from a 4- to 19-fold decrease in comparison to 19A. Superiority of the neutralizing potential of serum samples from convalescent vaccinated individuals over naïve vaccinated individuals was confirmed in a more physiologically representative HAE (human airway epithelium) model system exploiting primary human cells. In this assay, serum samples with comparable quantities of anti-RBD IgGs were tested for their neutralization capacity toward the 19A SARS-CoV-2 strain. We observed that serum samples collected from vaccinated convalescent individuals showed the highest neutralization capacity (Fig. 2D). This was regardless of anti-RBD IgG concentrations quantified previously in Fig. 1A, thus suggesting that Ig isotypes other than IgG also contribute to the neutralizing potential of these serum samples. Last, avidity of RBD-specific Abs in the different patient groups was measured using biolayer interferometry. Overall, RBD-specific Abs had higher avidity in vaccinated individuals as compared with convalescent unvaccinated patients, regardless of whether participants were infected before their vaccination (Fig. 2E and fig. S2F).

SARS-CoV-2 spike protein–specific CD4$^+$ T cells are differently polarized in convalescent vaccinated and naïve vaccinated individuals

Strong T cell responses were previously shown to inversely correlate with disease severity (*17*). Thus, monitoring of spike protein–specific T cell immunity is important for the assessment of protection against infection or reinfection. The memory T cell response against RBD peptides was first evaluated using a whole-blood interferon-γ (IFN-γ) release assay (*33*). The severe COVID-19 group was not included in this analysis to keep enough samples for subsequent mBC phenotyping studies. Results in Fig. 3A show the superiority of hybrid immunity for the T cell response as well. IFN-γ production was two- to fourfold higher in response to RBD peptides in the three convalescent vaccinated groups as compared with unvaccinated convalescents or the naïve BNT/BNT vaccinated group. The only difference between this T cell response profile and that of the Abs came from the ChAdOx/BNT-vaccinated group, which showed a production of IFN-γ comparable to that of individuals with hybrid immunity. This finding is consistent with our previous observation that a heterologous vaccination scheme induces a stronger T response than a homologous vaccination regimen at earlier time points (*34*). Whole-blood stimulation with membrane glycoprotein M peptides induced IFN-γ release in unvaccinated and vaccinated convalescent individuals only (Fig. 3B). To complete our analysis of the impact of prior SARS-CoV-2 infection on T cell responses to vaccination, we next conducted a comparative phenotypical analysis of spike protein–specific CD4$^+$ T cells in infection-naïve individuals vaccinated with two doses of BNT and convalescent patients vaccinated with one dose of BNT. The rationale for this choice was that individuals have been exposed twice to the SARS-CoV-2 spike protein in both groups. In these experiments, peripheral blood mononuclear cells were stimulated for 24 hours with a peptide pool derived from the spike protein. At the end of the culture, OX40 and CD137 were used as surface activation-induced

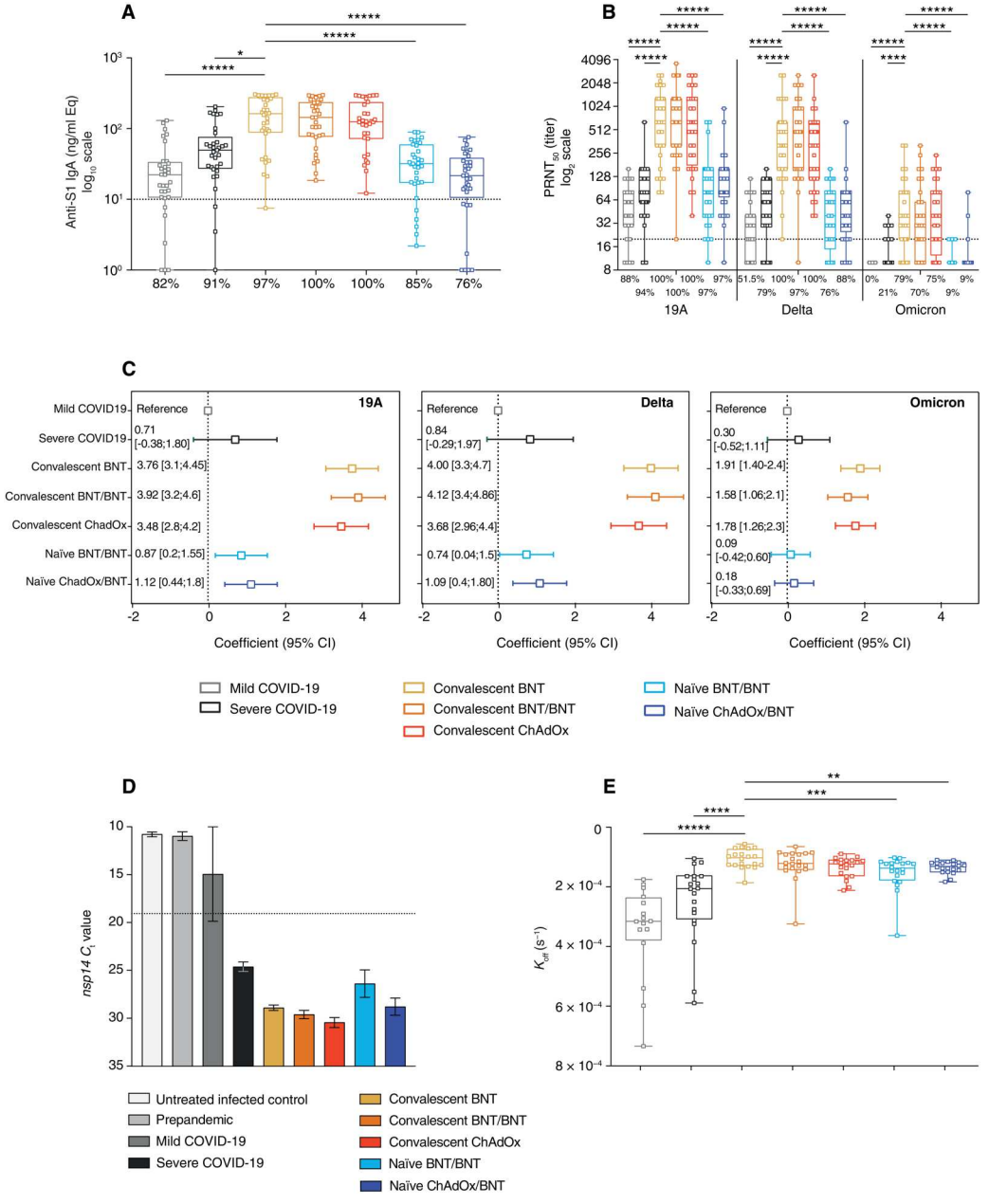

Fig. 2. Convalescent vaccinated individuals have high titers of SARS-CoV-2 spike protein–specific IgA and neutralizing Abs. (**A**) Serum samples from 33 individuals for each group (n = 32 for convalescent/ChAdOx individuals) were assayed for S1-specific IgA concentrations using custom-made enzyme-linked immunosorbent assays (ELISAs) at least 6 months after vaccination or infection. Concentrations are expressed in ng ml^{-1} equivalents of Ig. A log_{10} scale was used for the representation of the data. Each serum sample was evaluated in technical triplicate. (**B**) Serum samples were assayed in technical duplicate for their capacity to neutralize infection of Vero E6 cells by different SARS-CoV-2 strains. A log_2 scale was used for representation of the data. (**C**) The forest plots show the capacity of serum samples from the different groups to neutralize the 19A, Delta, and Omicron SARS-CoV-2 strains relative to the mild convalescent reference group after adjustment for age, sex, and delay between infection or vaccination and IgG measurement. The squares represent the regression coefficients, and bars indicate the 95% CI. (**D**) Two serum samples from each group with median anti-RBD IgG concentrations of 316.4 (IQR, 309.6 to 322.6) BAU/ml were tested in technical duplicate to assess their ability to neutralize the 19A SARS-CoV-2 strain in an HAE model. Two control conditions were performed: (i) prepandemic serum samples and (ii) untreated infected condition. At 72 hours after infection, SARS-CoV-2 replication was quantified in apical HAE supernatant by RT-PCR targeting the *nsp14* SARS-CoV-2 gene. C_t values are represented on the y axis. The dotted line represents the *nsp14* C_t value obtained after RT-PCR of the viral dilution used for these experiments. The histograms represent the mean values and SDs. (**E**) Total IgGs were purified from each individual serum sample (20 patients per group) and assayed for RBD-specific IgG off-rate measurement using biolayer interferometry at least 6 months after vaccination or infection. K_{off} values are expressed as s^{-1}. Each sample was evaluated as a single measurement. For (A), (B), and (E), data are expressed as box-and-whisker plots showing median (horizontal line inside the box), IQR (upper and lower horizontal lines of the box), and minimum and maximum (whiskers), and each dot corresponds to one individual. For (A) and (B), the dotted lines indicate the positive detection threshold. The percentages of samples above the positive threshold are indicated below the graphs. For the sake of clarity, statistical significance values are indicated for a limited number of comparisons. Complete matrices of statistical significance values are shown in fig. S2B [for (A)], fig. S2 (C to E) [for (B)], and fig. S2F [for (E)]. For all statistical analyses, *P < 0.05, **P < 0.01, ***P < 0.001, ****P < 0.0001, and *****P < 0.00001.

markers (AIMs) to estimate the frequency of spike protein–specific $CD4^+$ T cells as previously described (*35*). CXCR5 was used to discriminate T_{FH} cells ($CD4^+CXCR5^+$) from non-T_{FH} (T_H) ($CD4^+CXCR5^-$) $CD4^+$ T cells. As documented by Morita *et al.* (*36*), T_{FH} cells can be further subdivided into three subsets ($T_{FH}1$, $T_{FH}2$, and $T_{FH}17$) that can be delineated by their pattern of expression of the CXCR3 and CCR6 chemokine receptors. $T_{FH}1$, $T_{FH}2$, and $T_{FH}17$ are defined as $CXCR3^+CCR6^-$, $CXCR3^-CCR6^-$, and $CXCR3^-CCR6^+$, respectively. We observed no difference between the two groups of vaccinees regarding the frequencies of polyclonal and spike protein–specific T_{FH} and T_H cells (Fig. 3, C and D). By contrast, significantly (P < 0.05) increased frequencies of $T_{FH}1$ cells and decreased frequencies of $T_{FH}2$ were observed in the convalescent vaccinated group as compared with naïve vaccinated

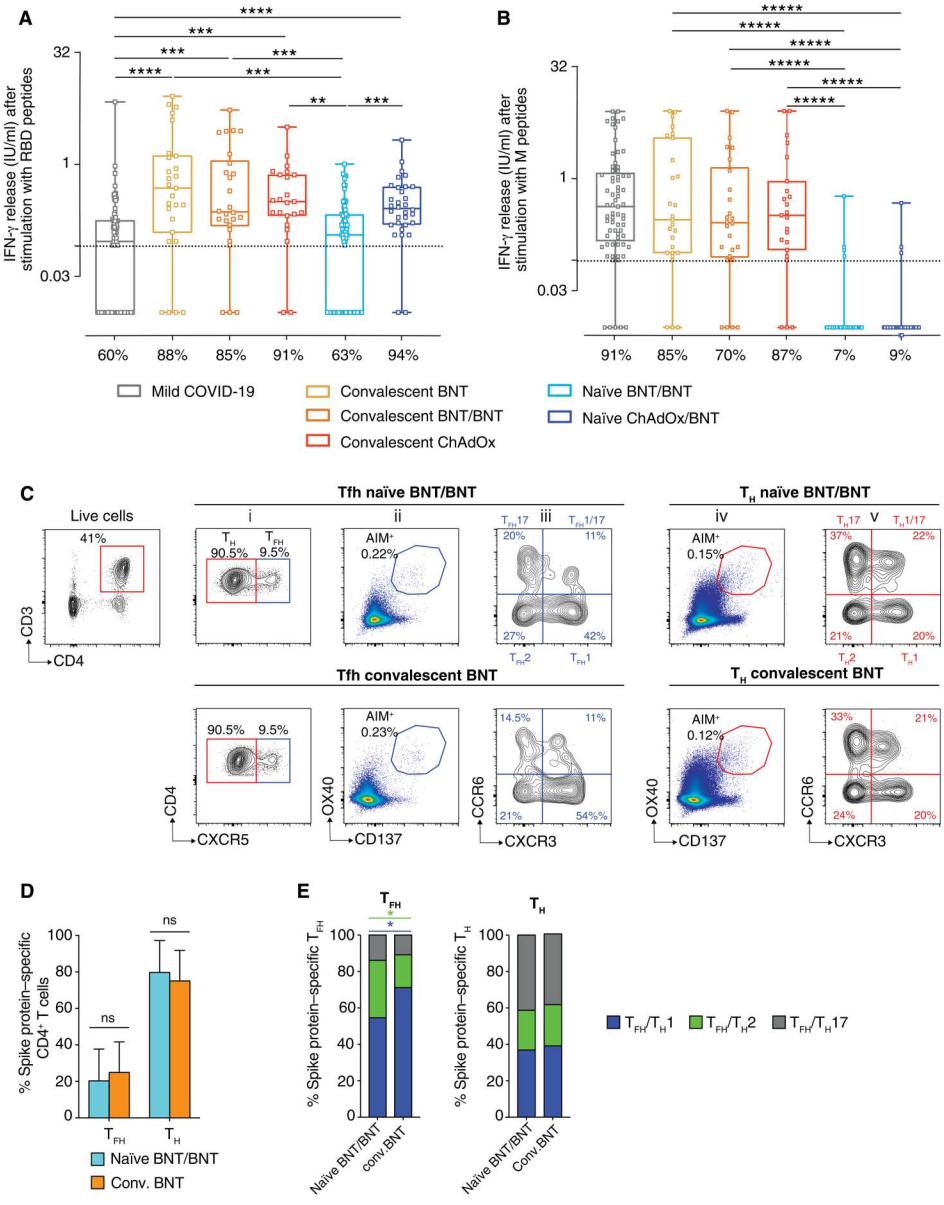

Fig. 3. T cell responses against SARS-CoV-2 spike protein are enriched in convalescent vaccinated individuals. (**A** and **B**) Whole blood cells from unvaccinated convalescent individuals after mild COVID-19 (n = 70), convalescent individuals vaccinated with one (n = 26) or two (n = 27) doses of the BNT vaccine or with the ChAdOx vaccine (n = 23), and naïve individuals vaccinated with two doses of BNT (n = 68) or with the ChAdOx/BNT combination (n = 32) were stimulated with RBD (A) or M peptides (B). For each stimulated condition, each sample was evaluated as a single measurement. IFN-γ release was measured by ELISA in the culture supernatants. Dotted lines indicate the positive detection threshold according to the manufacturer. Data are expressed as box-and-whiskers plots showing median (horizontal line inside the box), IQR (upper and lower horizontal lines of the box), and minimum and maximum (whiskers), and each dot corresponds to one individual. Statistical significance values of the data shown in (A) were derived from the adjusted model. The percentages of samples above the positive threshold are indicated below the graph. (**C**) Analysis of the $CD4^+$ T cell phenotype in naïve vaccinated individuals (BNT/BNT, top) and convalescent vaccinated individuals (BNT, bottom), with 10 samples for each group. Lymphocytes were pregated on the basis of morphology, CD45 expression, and exclusion of doublets and dead cells. $CD4^+$ T cells were then gated as shown (first contour plot on the left). Next panels, from left to right, are concatenated flow cytometry profiles illustrating the proportions of (i) T_H cells ($CD4^+$/$CXCR5^-$, red gate) and T_{FH} cells ($CD4^+CXCR5^+$, blue gate) among the entire $CD4^+$ T cell pool; (ii) non-naïve (AIM^+), spike protein–specific $CD4^+$ T_{FH} cells ($CD4^+CXCR5^+OX40^+CD137^+$) among the entire $CD4^+$ T cell pool; (iii) spike protein–specific $T_{FH}1$, $T_{FH}2$, $T_{FH}17$, and $T_{FH}1/17$ cells among spike protein–specific $CD4^+$ T_{FH} cells; (iv) non-naïve $CD4^+$ T_H cells ($CD4^+CXCR5^-OX40^{+-}CD137^+$); and (v) spike protein–specific T_H1, T_H2, T_H17, and $T_H1/17$ cells among spike protein–specific $CD4^+$ T_H cells. Values indicated on the graphs represent the frequencies of the indicated populations extracted from the gatings applied to the concatenated profiles. Data were background-subtracted against dimethyl sulfoxide–negative controls (cultures conducted without the peptide pool). (**D**) Bar graphs comparing the frequencies of spike protein–specific (AIM^+) $CD4^+$ T_H and T_{FH} cells in naïve vaccinated and convalescent vaccinated individuals. (**E**) Proportions of type 1, 2, and 17 spike protein–specific T_{FH} (left) and T_H (right) expressed as % of the type 1 + type 2 + type 17 spike protein–specific T_{FH}/T_H populations in naïve vaccinated and convalescent vaccinated individuals. In (E), the statistical significance of the intergroup differences is indicated on the graph in blue for $T_{FH}1$ and in green for $T_{FH}2$. A two-sided Pearson's chi-square test for equality of proportions was realized for statistical analysis in (E). The test was pairwise-realized and Bonferroni-corrected. For all statistical analysis, $^{**}P < 0.01$, $^{***}P < 0.001$, $^{****}P < 0.0001$, and $^{*****}P < 0.00001$; ns, nonsignificant.

individuals (Fig. 3E). Together, these results suggest that the enhanced vaccine-induced spike protein–specific Ab response of convalescent patients as compared with infection-naïve individuals is associated with increased $T_{FH}1$ polarization of their spike protein–specific T_{FH} cells but not with increased abundance of these cells.

Hybrid immunity is characterized by a remodeling of the SARS-CoV-2 RBD-specific mBC compartment

Analysis of the SARS-CoV-2 RBD-specific mBC compartment was conducted by multiparameter flow cytometry using fluorescently labeled tetrameric RBDs as previously described (*34*). Three mBC subsets were first defined by their pattern of expression of IgD and CD27 (fig. S3A): (i) IgD^+ mBCs (IgD^+CD27^+), also referred to as unswitched or innate mBCs; (ii) conventional switched mBCs (csM; IgD^-CD27^+); and (iii) DN mBCs (DN; IgD^-CD27^-), also referred to as atypical mBCs (*37*). The DN mBC population was then

further subdivided into DN1 ($CD21^+CD11c^-$) and DN2 ($CD21^-CD11c^+$) subtypes on the basis of the differential expression of CD21 and CD11c as previously described by Jenks and colleagues (*38*, *39*). Unsupervised analysis of the data was first carried out using the *t*-distributed stochastic neighbor embedding (*t*-SNE) algorithm applied to the staining files of the four most discriminant markers for separation of mBC subsets: IgD, CD27, CD21, and CD11c. Colored overlays of manually gated IgD^+, csM, DN1, and DN2 RBD-specific mBC subsets onto the *t*-SNE landscapes (Fig. 4A) show that the representation of DN2 mBCs, which is

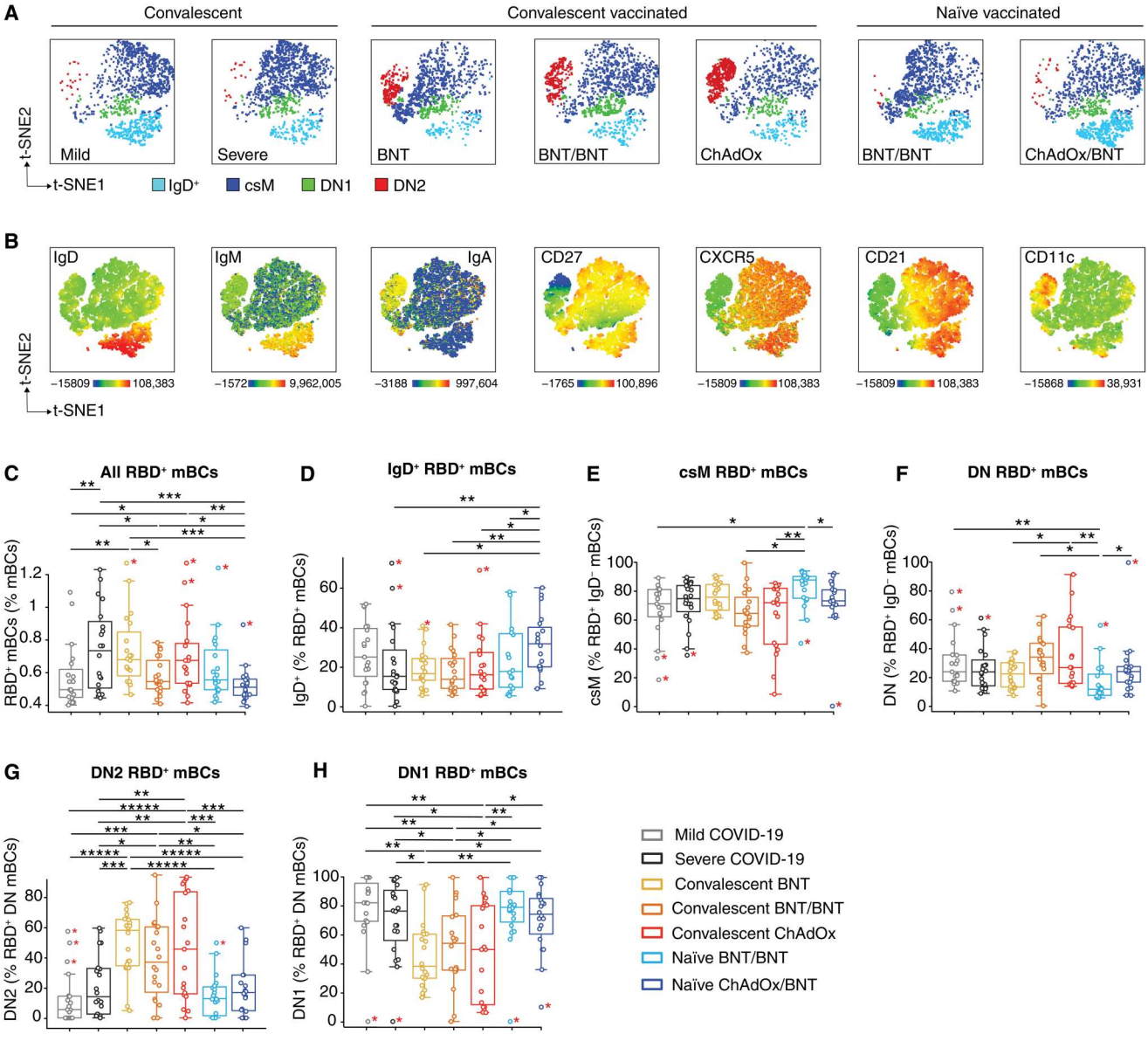

Fig. 4. The SARS-CoV-2 RBD-specific mBC pool differs between convalescent, convalescent vaccinated, and naïve vaccinated individuals. (**A**) *t*-SNE maps illustrate the RBD-specific mBC landscape for the seven groups of individuals. RBD-APC^+PE^+ events were exported as individual fcs files. The samples were then concatenated for *t*-SNE analysis. Each map corresponds to analysis of the merged files from 20 individuals. Four manually gated RBD^+ mBC subsets are overlaid on the *t*-SNE maps, and each subset is visualized with a distinct color code as indicated in the figure. (**B**) Expression of various markers used for mBC subset assignments is shown as heat plots on a consensus *t*-SNE map created after concatenation of all samples from the seven groups. The IgD^+ mBC area shows strong expression of IgD, IgM, CXCR5, CD21, and CD27; the csM area lacks expression of IgD and IgM but expresses CD27, CXCR5, and CD21; the DN1 area lacks IgD, CD11c, and CD27 expression but is $CXCR5^+$; the DN2 area lacks expression of IgD, CD21, CD27, and CXCR5 but is $CD11c^+$ and IgA^+. (**C** to **H**) Frequencies of the following RBD-binding mBCs are shown: (C) all RBD^+ mBCs (among polyclonal mBCs), (D) IgD^+ (among RBD^+ mBCs), (E) csM (among RBD^+ IgD^- mBCs), (F) DN (among RBD^+ IgD^- mBCs), (G) DN2 (among RBD^+ DN mBCs), and (H) DN1 (among RBD^+ DN mBCs). Each dot represents one individual ($n = 20$ individuals per group). Data are expressed as box-and-whiskers plots showing median (horizontal line inside the box), IQR (upper and lower horizontal lines of the box), and minimum and maximum (whiskers). Outliers are identified by red asterisks. We applied a beta regression model with the logit link function to assess statistical significance of intergroup differences regarding mBC subset frequencies. *$P < 0.05$, **$P < 0.01$, ***$P < 0.001$, and *****$P < 0.00001$.

marginal in the convalescent and naïve vaccinated individuals, is significantly ($P < 0.01$ to $P < 0.00001$) increased in the three groups of convalescent vaccinated individuals. Heatmaps of selected marker expression overlaid onto the *t*-SNE projections confirmed the identity of the four mBC subsets (Fig. 4B). The phenotypical characteristics of the RBD-specific mBC pool of convalescent, convalescent vaccinated, and naïve vaccinated individuals were next analyzed using conventional manual gating (fig. S3A). They are illustrated by the concatenated flow cytometry plots shown in fig. S3 (B to E) and by the box plot representations displayed in Fig. 4 (C to H). As shown in Fig. 4C, the frequencies of RBD-specific mBCs were significantly ($P < 0.05$ to $P < 0.001$) higher in convalescent vaccinated individuals than in naïve individuals vaccinated with the ChAdOx/BNT combination. However, they were not different from those found in unvaccinated individuals recovering from severe COVID-19 or from those of naïve individuals vaccinated with two doses of BNT. The frequencies of IgD^+ mBCs were reduced in the convalescent vaccinated groups as compared with naïve individuals vaccinated with the ChAdOx/BNT combination (Fig. 4D). csM were underrepresented in two groups of convalescent vaccinated individuals (BNT/BNT and ChAdOx/BNT) as compared with infection-naïve individuals vaccinated with the BNT/BNT combination (Fig. 4E). Conversely, DN mBCs were more abundant in convalescent vaccinated individuals than in naïve individuals vaccinated with the BNT/BNT combination (Fig. 4F). DN2 cells constituted the only mBC subtype, which followed exactly the same trend as the serum Ab (IgG and IgA) profiles in that the highest frequencies of RBD-specific DN2 mBCs were found in the groups of convalescent vaccinated individuals (Fig. 4G). The median frequency of DN2 mBCs for individuals with hybrid immunity was two- to threefold higher than that of naïve vaccinated individuals and two- to fivefold higher than that of previously infected unvaccinated individuals. As expected from their complementarity with DN2 cells among DN mBCs, frequencies of DN1 cells were inversely correlated with those of DN2 mBCs (Fig. 4H).

Together, these results indicate that RBD-specific mBCs are more abundant in convalescent vaccinated individuals as compared with naïve vaccinated individuals, but only for those who received the heterologous ChAdOx/BNT combination and compared with unvaccinated convalescents who recovered from mild (but not severe) COVID-19. The DN2 mBC subset is selectively expanded in convalescent vaccinated individuals with hybrid immunity. This singularity constitutes one of the parameters of cellular memory that distinguishes SARS-CoV-2 hybrid immunity from all other types of immunity.

Vaccination of COVID-19 convalescents increases the frequencies of IgA-switched RBD-specific mBCs

We next examined whether past infection history and vaccination regimen affected the proportions of isotype-switched RBD-specific mBCs. We identified IgA- and IgM-positive cells using isotype-specific Abs. For technical reasons, IgG-expressing cells were gated as IgM^-IgA^- B cells, a strategy that was validated by the fact that more than 90% of B cells falling in this gate expressed IgG (fig. S3F). Significantly ($P < 0.05$ and $P < 0.01$) higher frequencies of IgA-switched RBD-specific mBCs were found in convalescent vaccinated patients as compared with naïve vaccinated individuals, except for the convalescent BNT/BNT group, for which no difference was observed (Fig. 5A, left). By contrast, the frequencies of IgG-expressing mBCs were comparable in all groups, except for naïve individuals vaccinated twice with BNT, the frequencies for whom were significantly ($P < 0.05$) higher than those of the convalescent group after the same vaccination regimen (Fig. 5A, right). Next, our observation that the highest IgA expression on the *t*-SNE plots coincided with the area occupied by DN2 mBCs (Fig. 4, A and B) prompted us to explore further the links between IgA-switched RBD-specific mBCs and atypical mBCs. For this purpose, manually gated IgA^+ RBD^+ mBCs (red dots) were first projected onto the IgD/CD27 bi-parameter plot of the entire RBD-specific mBC population (blue dots) (Fig. 5B). We found that IgA-switched RBD-specific mBCs mostly belong to the csM or DN1 subsets (Fig. 5C). However, the abundance of IgA^+ mBCs belonging to the DN2 subtype was higher in unvaccinated convalescent individuals with past history of severe COVID-19, and in all three groups with hybrid immunity, as compared with naïve vaccinated individuals. The proportions of IgA-switched DN2 mBCs reached a maximum in the convalescent group vaccinated with ChAdOx, for which they represented nearly 50% of the IgA-expressing RBD-specific mBC pool. As observed for IgA^+ mBCs, the highest proportion of IgG-switched DN2 mBCs was also found for individuals with hybrid immunity (Fig. 5D), thus suggesting that the pathway responsible for generation of these atypical mBCs was not restricted to the mucosa-associated IgA isotype. Projection of manually gated IgA^+ DN RBD^+ mBCs (red dots) onto the CD21/CD11c bi-parameter plot of the entire RBD-specific atypical DN mBC population confirmed the prominence of cells with a DN2 memory phenotype among the pool of RBD-specific IgA^+ mBCs in convalescent vaccinated individuals (Fig. 5E). Together, our data indicate that hybrid immunity induces higher frequencies of IgA-switched mBCs than vaccine-induced immunity.

SARS-CoV-2 priming favors generation of atypical mBCs with a mucosal tropism

To examine the trafficking pattern of circulating switched RBD-specific mBCs, we first analyzed expression of the integrins α4β7 and α4β1, because they are critical for homing to the gut and airway mucosae, respectively, and of cutaneous lymphocyte antigen (CLA), a major skin-homing receptor (*40*, *41*). We also examined expression of CCR9, a marker that, among gut-committed cells, discriminates those that have a small intestine tropism ($CCR9^+$) from those committed to migrate to the colon ($CCR9^-$) (*42*). Although CLA was expressed by polyclonal T cells and a few polyclonal mBCs, it was undetectable on RBD-specific mBCs (fig. S4A). We obtained similar results with the skin-homing receptor CCR4 (*41*), which was undetectable on RBD-specific mBCs, thus suggesting that migration of RBD-specific mBCs to the skin is marginal. RBD-specific mBCs with an airway-homing potential ($\beta1^+\beta7^-$) were clearly dominant (more than two-thirds of the IgD^- RBD-specific mBC population) in all seven groups (Fig. 6A). Among RBD-specific mBCs with a gut-homing preference, the frequency of cells committed to migrate to the colon ($\beta1^+\beta7^+CCR9^-$) exceeded by far that of cells committed to migrate to the small intestine ($\beta1^+\beta7^+CCR9^+$) in all seven groups of participants (fig. S4B). To explore further the tissue-homing capacities of RBD-specific mBCs generated in different infection/vaccination contexts, we analyzed expression of the lymph node–homing receptors CD62L/L-selectin and CCR7 (*43*, *44*) on $\beta1^+\beta7^-$ and $\beta1^+\beta7^+$ RBD-specific mBCs from convalescent patients

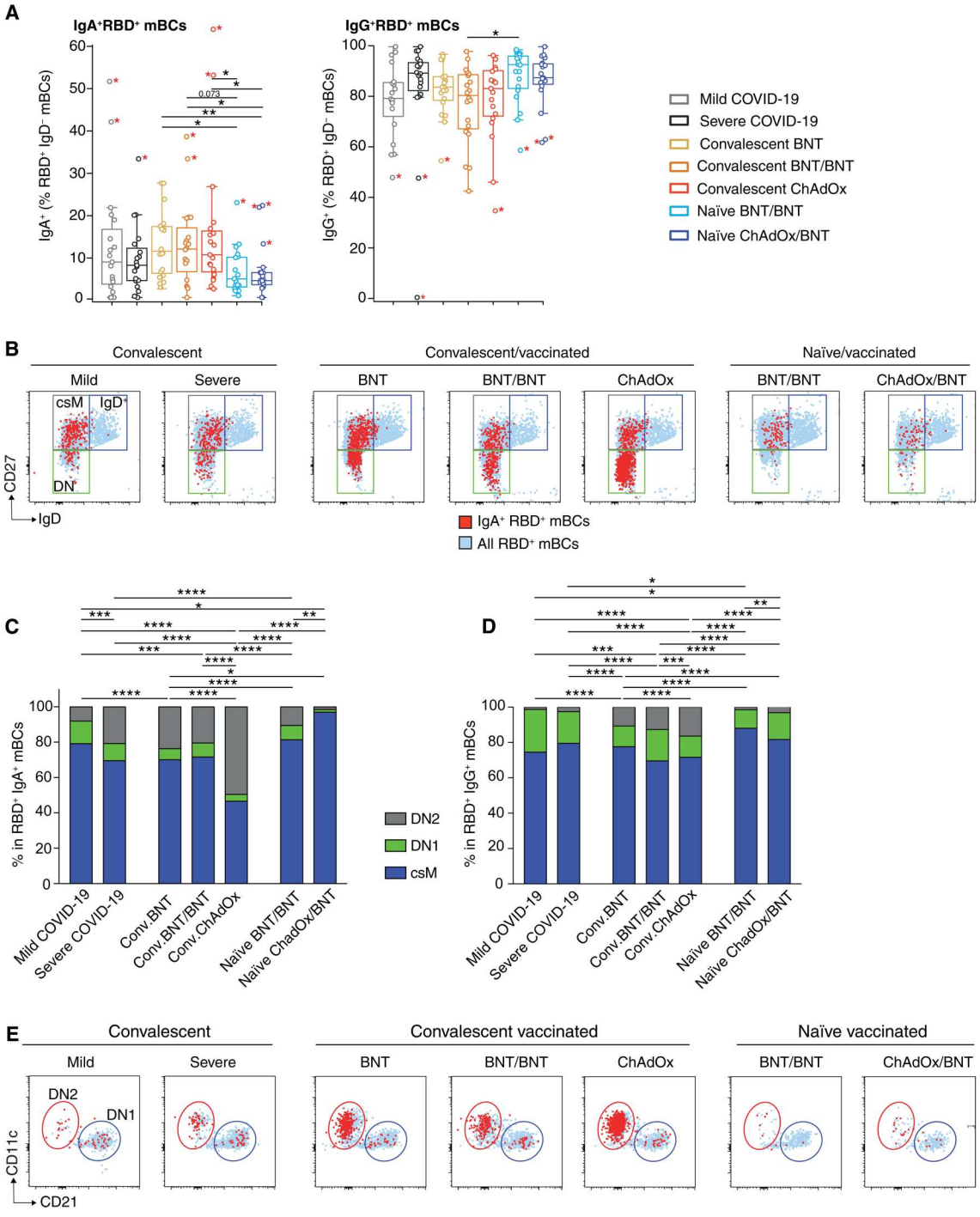

Fig. 5. Distribution of IgA- and IgG-switched B cells among SARS-CoV-2 RBD-specific mBC subsets varies on the basis of infection and vaccination status. (**A**) Frequencies of IgA^+ (left) and IgA^-IgM^- (designated here as IgG^+, right). RBD^+ mBCs expressed as percentages of the RBD^+IgD^- mBC population. Each dot represents one individual ($n = 20$ individuals per group). Data are expressed as box-and-whiskers plots showing median (horizontal line inside the box), IQR (upper and lower horizontal lines of the box), and minimum and maximum (whiskers). We applied a beta regression model with the logit link function to assess statistical significance of intergroup differences. $*P < 0.05$ and $**P < 0.01$. Outliers are indicated by red asterisks. (**B**) Visualization of the distribution of IgA^+RBD^+ mBCs within the csM and DN mBC subsets. Manually gated RBD^+ IgA^+ mBCs were overlaid (red dots) onto the IgD/CD27 bi-parameter plot of the entire RBD^+ mBC population (blue dots). (**C**) The proportions of RBD^+ IgA^+ mBCs belonging to the csM, DN1, and DN2 mBC subsets are shown expressed as % of the entire RBD^+ IgA^+ mBC pool. (**D**) The proportions of RBD^+ IgG^+ mBCs belonging to the csM, DN1, and DN2 mBC subsets are shown expressed as % of the entire RBD^+ IgG^+ mBC pool. For (C) and (D), the statistical significance of the intergroup differences regarding representation of the DN2 subset is indicated on the graph. A two-sided Pearson's chi-square test for equality of proportions was used for statistical analysis. The test was pairwise-realized and Bonferroni-corrected. $*P < 0.05$, $**P < 0.01$, $***P < 0.001$, and $****P < 0.0001$. (**E**) Distribution of RBD^+ IgA^+ DN mBCs among the DN1 and DN2 subsets. Manually gated RBD^+ IgA^+ DN mBCs were overlaid (red dots) onto the CD21/CD11c bi-parameter plot of the entire RBD^+ DN mBC population (blue dots).

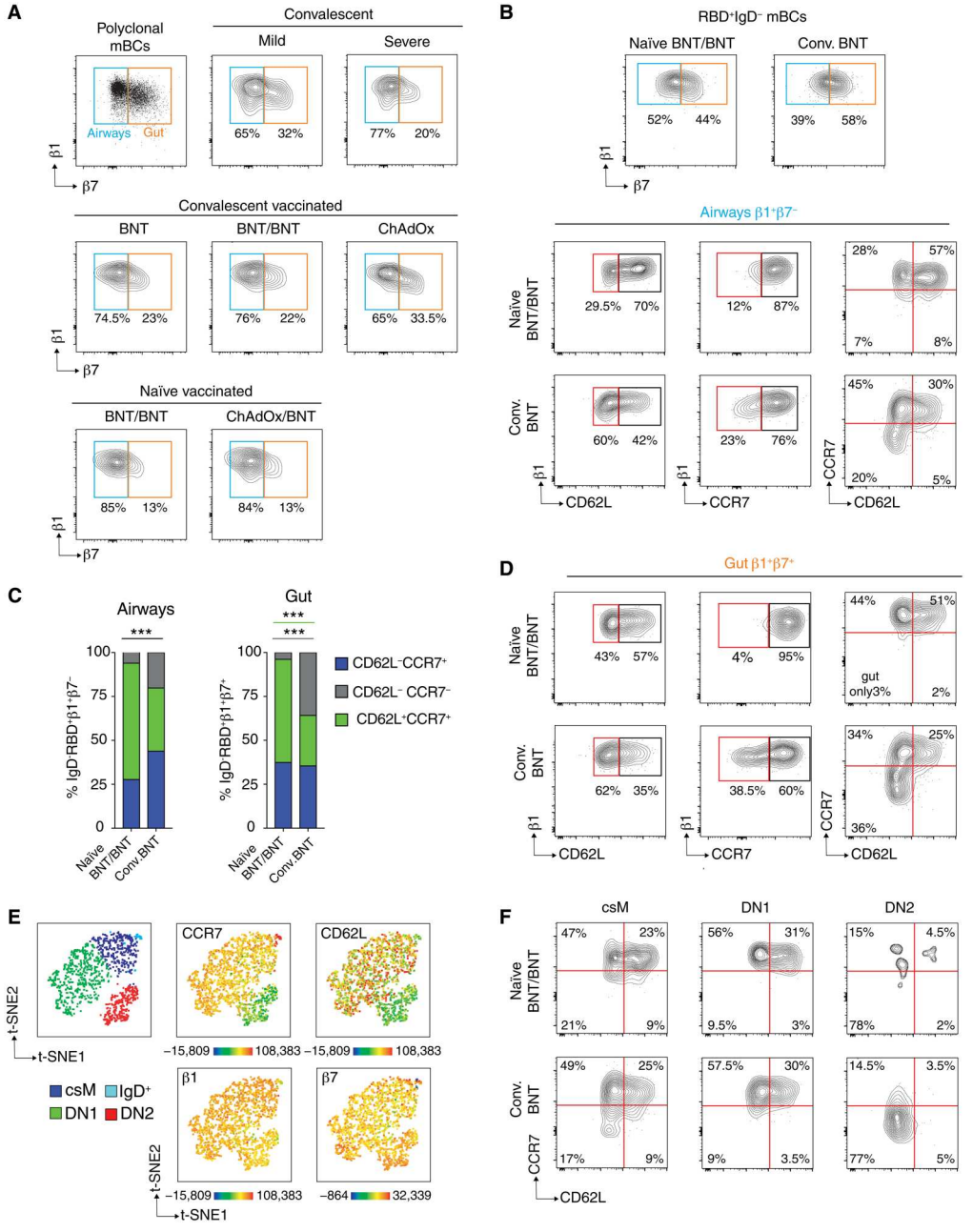

Fig. 6. Prior SARS-CoV-2 infection affects the homing potential of switched RBD$^+$ mBCs elicited by vaccination. (**A**) Pattern of expression of the β1 and β7 chains of integrins on RBD$^+$ switched mBCs in the seven groups of convalescent or vaccinated individuals. Airway-committed (β1$^+$β7$^-$) cells are highlighted by the blue gate, and gut-committed (β1$^+$β7$^+$) cells are highlighted by the orange gate. The flow cytometry profiles were obtained after concatenation of the fcs files from 10 individuals per group. The first plot on the left illustrates the β1/β7 expression profile of polyclonal mBCs from the convalescent vaccinated BNT/BNT group. (**B**) Pattern of expression of CD62L and CCR7 on airway-committed RBD-specific switched mBCs from naïve individuals vaccinated with the BNT/BNT combination (n = 19, middle) and convalescent individuals vaccinated with BNT (n = 14, bottom). The two contour plots at the top of (B) illustrate the gatings of β1$^+$β7$^-$ cells and β1$^+$β7$^+$ cells for naïve BNT/BNT (left) and convalescent/BNT individuals (right). (**C**) Comparison of the proportions of CD62L$^-$CCR7$^+$, CD62L^{+-} CCR7$^+$, and CD62L$^-$CCR7$^-$ B cells among airway-committed (left) and gut-committed (right) RBD-specific mBCs in naïve vaccinated and convalescent vaccinated individuals. (**D**) Same as (B) but for gut-committed RBD-specific switched mBCs. The flow cytometry profiles were obtained after concatenation of the fcs files from 19 and 14 individuals for the naïve vaccinated and convalescent vaccinated groups, respectively. (**E**) Left: t-SNE map illustrating the RBD-specific mBC landscape as obtained from the merged files of 19 individuals belonging to the naïve BNT/BNT group and 14 individuals from the convalescent BNT group. Manually gated, IgD$^+$, csM, DN1, and DN2 RBD$^+$ mBC subsets are overlaid onto the t-SNE maps, with each subset visualized by a distinct color code as indicated on the figure. The four other t-SNE maps visualize distribution of CCR7, CD62L, integrin β1, and integrin β7 shown as heat plots on the consensus t-SNE map illustrating the RBD$^+$ mBC landscape. (**F**) Pattern of expression of CCR7 and CD62L on csM, DN1, and DN2 RBD$^+$ mBC subsets gated as described in fig. S3. In (A), (B), (D), and (F), values indicated on the graphs represent the frequencies of the indicated RBD-specific B cell populations extracted from the gatings applied to the concatenated profiles. In (C), a two-sided Pearson's chi-square test for equality of proportions was used for statistical analysis. The test was pairwise-realized and Bonferroni-corrected. In (C) (left), the statistical significance value applies to all three populations. ***P < 0.001.

after a single dose of BNT vaccine and naïve individuals vaccinated twice with BNT. We found that a large proportion of β1$^+$β7$^-$ airway-committed RBD-specific mBCs also expressed combinations of the lymph node–homing receptors CD62L and CCR7 (Fig. 6B). The distribution of CCR7 and CD62L delineated three subtypes among the β1$^+$β7$^-$ RBD-specific mBC pool: CCR7$^+$CD62L$^-$, CCR7$^+$CD62L$^+$, and CCR7$^-$CD62L$^-$ cells. DN CCR7$^-$CD62L$^-$ mBCs were significantly (P < 0.001) more abundant in the convalescent vaccinated groups than in the naïve vaccinated group (Fig. 6C). Conversely, the frequency of double-positive CCR7$^+$ CD62L$^+$ mBCs was significantly (P < 0.001) lower in convalescent vaccinated than in naïve vaccinated individuals. The same conclusions applied to β1$^+$β7$^+$ gut-committed RBD-specific mBCs (Fig. 6, C and D), for which CCR7 and β1 were simultaneously expressed on virtually 100% of RBD-specific mBCs from naïve vaccinated individuals. We next measured the pattern of expression of CD62L, CCR7, and integrins β1/β7 by the different mBC subsets defined in Fig. 4. To do so, we first conducted an unsupervised analysis of

the data corresponding to the merged files of the 30 samples constituting the naïve BNT/BNT and convalescent/BNT groups using the *t*-SNE algorithm. As described previously (Fig. 4), expression of the IgD, CD27, CD21, and CD11c markers allowed for the creation of an RBD-specific mBC landscape on which we could visualize IgD^+, csM, DN1, and DN2 mBC subsets (Fig. 6E, top left plot). Heatmaps of homing receptor expression overlaid onto the *t*-SNE plot (Fig. 6E) revealed that the DN2 subset was the only mBC subtype that lacked expression of the lymph node–homing receptors CCR7 and CD62L. To confirm these data, we separately gated the three switched RBD-specific mBC subsets (csM, DN1, and DN2) and used bi-parameter plots to visualize their expression of CCR7 and CD62L. We found that most DN2 mBCs differed from csM and DN1 mBCs by their lack of CCR7 and CD62L expression (Fig. 6F). Because the β1 chain of integrins is homogeneously expressed on all RBD-specific mBCs (Fig. 6A), we are confident that CCR7/CD62L DN mBCs express at least one of the integrin β chains that confer mucosal tropism. In agreement with our observation that DN2 cells were expanded only in individuals with hybrid immunity, very few RBD-specific DN2 cells were found in the naïve vaccinated group.

Together, our data show that a large proportion of RBD-specific mBCs express a joint tropism for mucosal sites and peripheral lymphoid tissues. However, only individuals with hybrid immunity display RBD-specific mBCs with an exclusive mucosal tropism, which, in their great majority, belong to the DN2 memory subtype. These data suggest that SARS-CoV-2 virus infection imprints an mBC differentiation program that allows for expansion of an atypical mBC subset with an exclusive mucosal homing potential upon subsequent vaccination.

Serological and cellular markers of SARS-CoV-2 spike protein–specific mBC correlate with one another

We next asked whether serological and cellular markers of infection- and vaccination-elicited memory correlate with each other. To address this question, we first evaluated a matrix analysis that integrated both the serological memory data (titers of IgG and IgA Abs, neutralization potential) and the cellular memory data (frequencies of diverse RBD-specific mBC subsets). This analysis revealed a strong positive correlation between the frequencies of DN2 mBCs and the serum titers of anti-S1 IgA, anti-RBD IgG Abs, and serum neutralization potential against the SARS-CoV-2 19A strain (B38 lineage) (Fig. 7A). These data also indicated a correlation between the neutralization potential of serum and serum titers of RBD-specific IgGs and S1-specific IgAs.

We next constructed restricted correlation matrices that integrated only the frequency of DN2 and IgA-expressing RBD-specific mBCs and serological parameters. This time, data from convalescent, convalescent vaccinated, and naïve vaccinated individuals were analyzed separately. The positive correlation previously observed between the frequency of DN2 mBCs and the titers of anti-S1 IgA Abs when all samples from the seven experimental groups were merged was lost when the tests were conducted separately on the three groups of individuals described above (Fig. 7B). However, the correlation between DN2 mBC frequency, on the one hand, and anti-RBD IgG titers and neutralization potential, on the other hand, remained positive but only for the individuals from the hybrid immunity group. By contrast, positive correlation between the anti-spike protein IgA titers and virus neutralization potential appeared to be restricted to the convalescent group. Together, these findings suggest that for convalescent vaccinated individuals, the differentiation pathway that leads to generation of DN2 mBCs is associated with development of serum anti-spike protein IgG Abs and with virus neutralization potential of the serum. They also suggest that for convalescent individuals, the IgA isotype also contributes to the virus neutralization activity of the serum.

DISCUSSION

Cellular mBC has been somewhat overlooked in the vast literature devoted to vaccine-induced immunity against SARS-CoV-2, which instead focused on the parameters of serological memory. It is nevertheless vital for protection against viral escape mutants, as documented in different contexts of viral infection. For example, it has been reported early on in a West Nile virus murine infection model that mBCs recognize variants of the original pathogen more efficiently than the Abs produced by long-lived plasma cells (PCs) (*45*). This has been recently confirmed in humans in the context of SARS-CoV-2 by Kotaki and colleagues (*46*), who showed that, in vaccinated individuals, broadly reactive Ab specificities that recognize the Delta and Omicron SARS-CoV-2 variants are poorly represented in the sera of vaccinees but are preserved in their mBC pool. These considerations gave us the incentive to undertake a comprehensive analysis of both serological and cellular B cell immunity generated by SARS-CoV-2 infection or by an mRNA or adenovirus-based vaccine delivered to SARS-CoV-2–naïve or previously infected individuals.

Collectively, our results underscore that vaccination of previously infected patients is required to optimize their immune protection against SARS-CoV-2 reinfection. As previously pointed out for the humoral response against the varicella zoster (*47*) and influenza (*48*) viruses, we show here that hybrid immunity conferred by a combination of infection and vaccination (in the context of different vaccine regimens) is superior to immunity conferred by infection or vaccination alone, as far as long-term serum Ab responses are concerned. Regarding cellular memory, quantitative superiority of hybrid immunity is less clear-cut, except for DN2 mBCs that follow exactly the same trend as the spike protein–specific Ab response. In particular, the frequencies of RBD-specific mBCs in naïve and convalescent individuals vaccinated with BNT are similar, whatever the number of doses administered to convalescents. This suggests that prior exposure to the virus does not confer a numerical advantage in terms of cellular mBC as compared with a two-dose vaccination regimen with BNT applied to infection-naïve individuals. We can only speculate on the biological cues that underlie the discrepancy between serological and cellular mBC in individuals with hybrid immunity, but one possible scenario could be that viral infection (as opposed to vaccination) preferentially generates PC-committed mBCs. It is now widely accepted that the mBC pool encompasses at least two subtypes that are predetermined to either differentiate into PCs or form germinal centers (GCs) and reconstitute the mBC compartment, at least in murine models (*49*–*51*). In this context, DN2 mBCs, described to be committed to a PC cell fate (*38*), are amplified in convalescent vaccinated individuals, and their frequency positively correlates with the anti-spike protein IgG serum titers in this group of vaccinees. This fits with the possibility that viral infection could promote skewing of the mBC output toward PC-committed mBC clones.

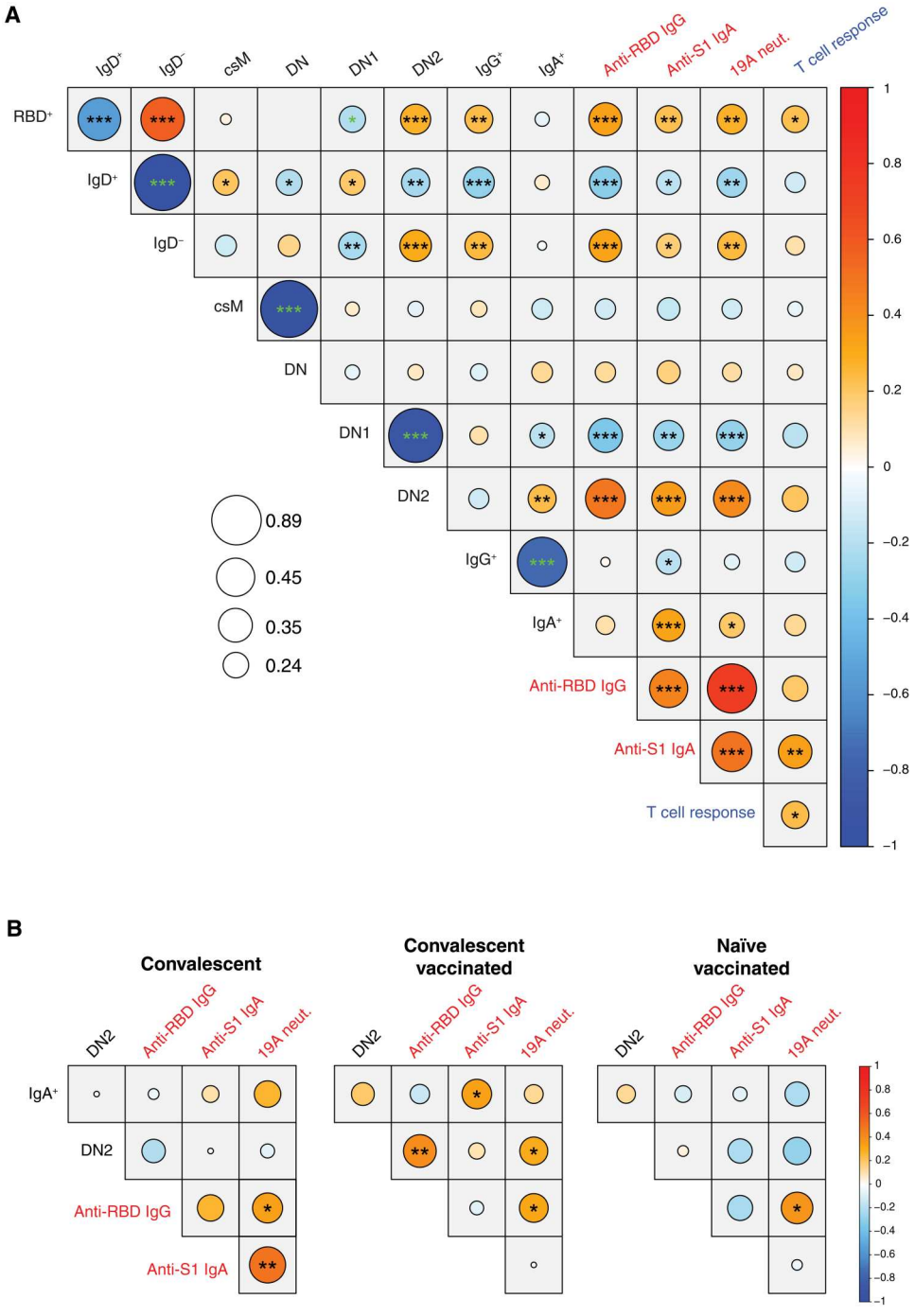

Fig. 7. Analysis of interrelationships between serologic and cellular immune memory parameters. (**A**) A matrix file that contains the merged serological and cellular immune measurements for all groups of individuals was created. Correlations between each pair of variables were calculated by the Spearman nonparametric method. The size and color intensity of the circles correspond to values of the correlation factor rho (legend on the graph), and the stars indicate statistical significance of the correlation (*$P < 0.05$, **$P < 0.01$, and ***$P < 0.001$). Serological and cellular mBC parameters are indicated in red and black, respectively. The T cell response is indicated in blue and corresponds to the IFN-γ release values in response to RBD stimulation, expressed in IU/ml. Anti-RBD IgG and anti-S1 IgA correspond to the serum titers expressed as BAU/ml and ng/ml, respectively. Neutralization (neut.) corresponds to the neutralizing activity of the serum against the 19A SARS-CoV-2 strain expressed as $PRNT_{50}$ titers. (**B**) A limited correlation analysis was conducted separately on the merged samples from three groups of individuals: convalescent (mild + severe COVID-19), convalescent vaccinated (BNT + BNT/BNT + ChAdOx vaccinations), and naïve vaccinated (BNT/BNT + ChAdOx/BNT). The correlation matrices are restricted to five parameters (% IgA^+ mBCs, % DN2 mBCs, anti-RBD IgG titers, anti S1 IgA titers, and neutralization potential against the 19A SARS-CoV-2 strain).

On the whole, our data support the hypothesis that prior virus exposure initiates changes in the mBC landscape, as illustrated by the increased abundance of the atypical memory DN2 mBC subset induced in convalescent individuals by vaccination. The latter observation is in agreement with the results of Sokal and colleagues (*52*), who reported that vaccination expands RBD-specific DN2 cells in both mild and severe COVID-19 patients. Development of DN2 mBCs is known to be driven by IFN-γ, interleukin-21 (IL-21), and ligands of Toll-like receptors 7 and 8 (*38*), which are all produced in the context of viral infection. In keeping with this, we show here, in agreement with Rodda and colleagues (*53*), that hybrid immunity is also associated with enhanced $T_{FH}1$ polarization of spike protein–specific $CD4^+$ T cells, which likely translates into enhanced IFN-γ production. This observation is also in agreement with the results of the interferon-gamma release assay (IGRA) test (Fig. 3A) showing that the highest amounts of IFN-γ production by spike protein–specific T cells were found in convalescent vaccinated individuals. IFN-γ has been described to induce T-bet (T-box expressed in T cells) expression in B cells (*54*) and to promote in vitro development of $T\text{-bet}^{hi}$ pre–Ab-secreting cells with a DN2 phenotype (*55*). We would thus like to propose that the $T_{FH}1$-enriched environment in convalescent vaccinated individuals may contribute to expansion of DN2 mBCs that characterize hybrid immunity.

The identity of DN2 cells is still debated. They were presented as mBCs of extrafollicular origin by Sanz *et al.* (*37*) and Jenks *et al.* (*38*), and examination of secondary lymphoid tissues of severely ill COVID-19 patients revealed an increased representation of DN2 mBCs concomitant with a collapse of GCs, T_{FH}, and GC B cells (*56*). Our observation that the follicular homing receptor CXCR5, which is expressed on IgD^+, csM, and DN1 mBCs, is lacking on RBD-specific DN2 cells is an argument in favor of their extrafollicular origin. It remains that induction of CD11c and down-regulation of CD21 can also occur on various B cell subsets as the result of activation (*37*). In keeping with this, spike protein–specific mBCs with a $CD11c^+CD21^-$ phenotype in severe COVID-19 patients have been documented to segregate together with other activated B cell subsets in a cluster of $CD71^{+/lo}$ activated mBCs after dimensional reduction analysis (*57*). Still, description of mBCs generated independently of the GC reaction in a context of viral infection is not totally unprecedented, because it was documented that more than half of the lung influenza–specific mBCs induced by pulmonary influenza virus infection in mice lack expression of the GC-related marker CD73 (*58*). It is legitimate to ask whether expansion of DN2 mBCs is beneficial or detrimental to SARS-CoV-2–induced immunity. Until now, DN2 mBCs have mostly been considered to be pathogenic, with the best documented example found in patients with systemic lupus erythematosus, in whom these cells contribute to the disease because of their autoreactive specificities (*59*). On the other hand, would their extrafollicular origin be confirmed, these cells could provide better cross-protection against viral escape mutants because GC-independent mBCs have been reported to display a more broadly reactive Ab repertoire (*60*, *61*).

Besides amplification of DN2 mBCs, increased abundance of IgA-switched RBD-specific mBCs was another distinctive feature of hybrid immunity (at least for the BNT and ChAdOx groups) when compared with vaccine-induced immunity in infection-naïve individuals. IgA is a crucial component of the immune response at mucosal surfaces, including the upper respiratory tract, which is the main portal of entry for SARS-CoV-2 (*62*, *63*). It is therefore not surprising that SARS-CoV-2 infection allows for generation of higher frequencies of IgA-bearing mBCs than systemic vaccination. Besides expansion of IgA-expressing mBCs, the hypothesis of an enhanced mucosal response in individuals with hybrid immunity is further supported by analysis of the homing pattern of RBD-specific mBCs. First, we demonstrated that all RBD-specific mBCs, irrespective of the infection/vaccination context, express the β1 or β7 chain of integrins that are critical determinants of mucosal homing imprinting, with a clear dominance of an airway-homing signature. The latter observation is coherent with the study of Müller and colleagues (*64*) reporting reduction of α4β7-expressing memory T cells in COVID-19 patients, including those presenting with intestinal symptoms. Because circulating mBCs have been reported to return to the tissue where they were originally generated (*65*), our present finding suggested that mucosae of the upper respiratory tract would be prominent sites for induction of mBC not only in the context of infection but also in response to parenteral vaccination. This observation was even more notable considering that the mRNA-based BNT vaccine is described to be a poor inducer of mucosal immunity (*66*). However, a more detailed examination of the homing signature of RBD-specific mBCs revealed that a sizeable proportion of RBD-specific mBCs have a complex trafficking pattern characterized by coexpression of mucosal (β chains of integrins) and systemic (CCR7 and CD62L) homing receptors. It is conceivable that this dual homing profile confers to RBD-specific mBCs the capacity to distribute in both mucosal and peripheral lymphoid tissues. Such a joint tropism has been previously documented for Ab-secreting cells in the context of enteric infections caused by *Vibrio cholerae* (*67*) and in volunteers immunized by the mucosal or systemic routes with a cholera toxin B–containing cholera vaccine (*68*). Moreover, this phenotypical analysis also revealed the existence of a population of DN ($CD62L^-$ $CCR7^-$) RBD-specific mBCs that expressed only β chains of integrins; this population was almost exclusively present in convalescent vaccinated individuals. Unexpectedly, our data indicate that this RBD-specific subset is almost entirely constituted of DN2 mBCs. This leads us to propose that DN ($CCR7^-$/$CD62L^-$) DN2 RBD-specific mBCs display an exclusive mucosal tropism that may be able to afford protection at the sites of viral entry. This hypothesis is also consistent with the observation that hybrid immunity confers higher protection than vaccination alone against breakthrough SARS-CoV-2 infections (*69*).

One of the potential limitations of our work is the limited number of individuals included in this study for phenotypical analysis of RBD-specific mBCs ($n = 20$), analysis of their homing potential (19 and 14 individuals for the naïve vaccinated and convalescent vaccinated groups, respectively), and phenotypical analysis of spike protein–specific $CD4^+$ T cells ($n = 10$), which lowers the power of the statistical analysis. In addition, assessment of the homing potential of recirculating mBCs is only a surrogate estimation of the size of the physiologically relevant pool of mucosa-resident RBD-specific mBCs. Definite proof that hybrid immunity confers better immune protection at the mucosal sites of entry of the virus would require further analysis, such as assessment of dimeric IgA in bronchoalveolar lavages or saliva. Last, our experimental approach did not allow us to compare conventional and DN2 mBCs for their SARS-CoV-2 neutralization capacity (including against VOCs). It

remains to be assessed whether unconventional DN2 mBCs, which constitute a signature of hybrid immunity, are beneficial to immune protection against SARS-CoV-2 and its viral escape mutants.

Together, our data establish that SARS-CoV-2 infection followed by vaccination more efficiently primes the immune system than vaccination alone and builds superior serological and mBC responses, including at airways and gut mucosal sites. The superiority of hybrid immunity was correlated with expansion of an atypical DN2 mBC subtype that displayed a mucosal-restricted tropism. These data support the inclusion of previously infected people in SARS-CoV-2 booster vaccination campaigns.

MATERIALS AND METHODS

Study design

For the Covid-Ser cohort, clinical data were recorded by a trained clinical research associate using Clinsight software (version _ Csonline 7.5.720.1). Blood samples were processed and stored at the Centre de Ressource Biologique Neurobiotec, 69500 Bron. Seven hundred and fourteen naïve health care workers (HCWs) infected with SARS-CoV-2, vaccinated against SARS-CoV-2, or both were included in a prospective longitudinal cohort study conducted in Hospices Civils de Lyon (HCL; Lyon, France). Blood sampling was performed 6 months after the end of vaccination schedule or infection. Concerning naïve vaccinated HCWs, the absence of previous SARS-CoV-2 infection was confirmed using the Wantai Ab total assay in the prevaccine sample. The Wantai SARS-CoV-2 total Ab assay, detecting anti-RBD Abs, was selected to detect a previous infection before vaccination on the basis of its better sensitivity in infected individuals as compared with other commercial qualitative assays we had evaluated in a previous study (*70*). SARS-CoV-2 infection before vaccination occurred during the first wave of the pandemic, before the emergence of VOCs. Infected patients were considered to have a mild form of COVID-19 if they were symptomatic but did not require hospitalization. Written informed consent was obtained from all participants; ethics approval was obtained from the national review board for biomedical research in April 2020 (Comité de Protection des Personnes Sud Méditerranée I, Marseille, France; ID RCB 2020-A00932-37), and the study was registered on ClinicalTrials.gov (NCT04341142). The inclusion criteria for this study were as follows: (i) seropositive HCWs screened for anti–SARS-CoV-2 Abs; (ii) be at least 18 years of age; (iii) HCWs having given their written consent and accepting a follow-up every 6 months; and (iv) HCWs affiliated to a social security scheme or beneficiary of such a scheme. The exclusion criterion of this study was pregnant or lactating woman.

The Immunonosocor cohort is an extension of the NOSOCOR project registered as ClinicalTrials: NCT04637867. Hospitalized patients were considered to have a severe form of COVID-19 if their hospital stay was longer than 24 hours. In our cohort, the median (IQR) duration of the hospital stay was 10 (5.5 to 20) days, and 36 of 183 (19.7%) patients were admitted into the intensive care unit. The clinical research and ethics committee of Ile de France V approved the study on 14 October 2020 (no. 20.02.27.69817 Cat 3). Inclusion criteria for this study were (i) SARS-CoV-2 confirmed by reverse transcription polymerase chain reaction (RT-PCR), (ii) adults at least 18 years of age, (iii) signed consent form, and (iv) adults affiliated with the French health system. Exclusion criteria for this study were (i) pregnant women, (ii) hospitalized patients, (iii) adults subject to legal protection, (iv) imprisoned adults, and (v) adults who have expressed an opposition to participate or who do not wish to donate blood samples. One hundred and eighty-three patients hospitalized for severe COVID-19 in HCL settings during the first wave of the pandemic were included in the NOSOCOR study. Twenty-five percent of them required ventilation. Blood samples were collected from all patients at least 6 months after the initial SARS-CoV-2 infection. Demographic characteristics are depicted in Table 1.

Statistical analysis

Raw, individual-level data for experiments where $n < 20$ are presented in data file S1. The outcomes of interest were immune parameters measured between 6 and 8 months on average after the last immune stimulation—either infection or vaccine. Statistical analyses were carried out identically for each immune variable studied. All groups were first described with box-and-whiskers plots. To take into account confounding factors, we fitted a multivariate linear regression model, adjusting the group effect for the age, sex, and delay covariates. The *P* values shown on box-and-whiskers plots were derived from the adjusted model. Log_2 transformation of the immune variable was applied to approach the assumptions of the linear model. Quadratic effect of age was tested and retained in the model when it was significant. Model diagnoses were performed to check underlying assumptions, and special attention was paid to the standardized residuals. The analyses were performed with R software (https://cran.r-project.org/). Our predictors were age, as a continuous variable (considered as a possible confounder), sex, and the vaccination regimen, whereby convalescent = 0 and naïve = 1.

For determination of the statistical significance of intergroup differences regarding mBC subset frequencies (Figs. 4, C to H, and 5A), we used beta regression modeling because our outcome variable is doubly bounded on the (0,1) interval. This approach uses an error structure appropriate for proportion data assuming that the dependent variable follows the beta distribution. In addition, using the logit link, parameter estimates resulting from our model allow for a better interpretation of the differences between groups because both magnitude and direction of group effect can be accurately quantified. A two-sided Pearson′s chi-square test for equality of proportions was applied for intergroup comparisons of the proportions of DN2 mBCs among the RBD^+ IgA^+ and IgG^+ compartments (Figs. 5, C and D, and 6C). The test was pairwise-realized and Bonferroni-corrected. Our null hypothesis was that the proportion of DN2 mBCs (considered as success probability) was the same in the two compared experimental groups. For the correlation matrix shown in Fig. 7, the correlation between each pair of variables was calculated by the Spearman nonparametric method. Missing values were managed as follows: In each two variables being correlated, we used all complete pairs of observations on those variables; thus, we could take advantage of all available data in our study.

Supplementary Materials

This PDF file includes:

Materials and Methods
Figs. S1 to S4
References (*71–73*)

Other Supplementary Material for this manuscript includes the following:
Data file S1
MDAR Reproducibility Checklist

View/request a protocol for this paper from *Bio-protocol*.

REFERENCES AND NOTES

1. M. B. Shenai, R. Rahme, H. Noorchashm, Equivalency of protection from natural immunity in COVID-19 recovered versus fully vaccinated persons: A systematic review and pooled analysis. *Cureus* **13**, e19102 (2021).
2. N. Kojima, N. K. Shrestha, J. D. Klausner, A systematic review of the protective effect of prior SARS-CoV-2 infection on repeat infection. *Eval. Health Prof.* **44**, 327–332 (2021).
3. F. P. Polack, S. J. Thomas, N. Kitchin, J. Absalon, A. Gurtman, S. Lockhart, J. L. Perez, G. Pérez Marc, E. D. Moreira, C. Zerbini, R. Bailey, K. A. Swanson, S. Roychoudhury, K. Koury, P. Li, W. V. Kalina, D. Cooper, R. W. Frenck, L. L. Hammitt, Ö. Türeci, H. Nell, A. Schaefer, S. Ünal, D. B. Tresnan, S. Mather, P. R. Dormitzer, U. Şahin, K. U. Jansen, W. C. Gruber; C4591001 Clinical Trial Group, Safety and efficacy of the BNT162b2 mRNA covid-19 vaccine. *N. Engl. J. Med.* **383**, 2603–2615 (2020).
4. M. N. Ramasamy, A. M. Minassian, K. J. Ewer, A. L. Flaxman, P. M. Folegatti, D. R. Owens, M. Voysey, P. K. Aley, B. Angus, G. Babbage, S. Belij-Rammerstorfer, L. Berry, S. Bibi, M. Bittaye, K. Cathie, H. Chappell, S. Charlton, P. Cicconi, E. A. Clutterbuck, R. Colin-Jones, C. Dold, K. R. W. Emary, S. Fedosyuk, M. Fuskova, D. Gbesemete, C. Green, B. Hallis, M. M. Hou, D. Jenkin, C. C. D. Joe, E. J. Kelly, S. Kerridge, A. M. Lawrie, A. Lelliott, M. N. Lwin, R. Makinson, N. G. Marchevsky, Y. Mujadidi, A. P. S. Munro, M. Pacurar, E. Plested, J. Rand, T. Rawlinson, S. Rhead, H. Robinson, A. J. Ritchie, A. L. Ross-Russell, S. Saich, N. Singh, C. C. Smith, M. D. Snape, R. Song, R. Tarrant, Y. Themistocleous, K. M. Thomas, T. L. Villafana, S. C. Warren, M. E. E. Watson, A. D. Douglas, A. V. S. Hill, T. Lambe, S. C. Gilbert, S. N. Faust, A. J. Pollard; Oxford COVID Vaccine Trial Group, Safety and immunogenicity of ChAdOx1 nCoV-19 vaccine administered in a prime-boost regimen in young and old adults (COV002): A single-blind, randomised, controlled, phase 2/3 trial. *Lancet* **396**, 1979–1993 (2021).
5. C. Manisty, A. D. Otter, T. A. Treibel, Á. McKnight, D. M. Altmann, T. Brooks, M. Noursadeghi, R. J. Boyton, A. Semper, J. C. Moon, Antibody response to first BNT162b2 dose in previously SARS-CoV-2-infected individuals. *Lancet* **397**, 1057–1058 (2021).
6. S. E. Racine-Brzostek, J. K. Yee, A. Sukhu, Y. Qiu, S. Rand, P. D. Barone, Y. Hao, H. S. Yang, Q. H. Meng, F. S. Apple, Y. Shi, A. Chadburn, E. Golden, S. C. Formenti, M. M. Cushing, Z. Zhao, Rapid, robust, and sustainable antibody responses to mRNA COVID-19 vaccine in convalescent COVID-19 individuals. *JCI Insight* **6**, e151477 (2021).
7. S. Havervall, U. Marking, N. Greilert-Norin, H. Ng, M. Gordon, A.-C. Salomonsson, C. Hellström, E. Pin, K. Blom, S. Mangsbo, M. Phillipson, J. Klingström, S. Hober, P. Nilsson, M. Åberg, C. Thålin, Antibody responses after a single dose of ChAdOx1 nCoV-19 vaccine in healthcare workers previously infected with SARS-CoV-2. *EBioMedicine* **70**, 103523 (2021).
8. R. Keeton, S. I. Richardson, T. Moyo-Gwete, T. Hermanus, M. B. Tincho, N. Benede, N. P. Manamela, R. Baguma, Z. Makhado, A. Ngomti, T. Motlou, M. Mennen, L. Chinhoyi, S. Skelem, H. Maboreke, D. Doolabh, A. Iranzadeh, A. D. Otter, T. Brooks, M. Noursadeghi, J. C. Moon, A. Grifoni, D. Weiskopf, A. Sette, J. Blackburn, N.-Y. Hsiao, C. Williamson, C. Riou, A. Goga, N. Garrett, L.-G. Bekker, G. Gray, N. A. B. Ntusi, P. L. Moore, W. A. Burgers, Prior infection with SARS-CoV-2 boosts and broadens Ad26.COV2.S immunogenicity in a variant-dependent manner. *Cell Host Microbe* **29**, 1611–1619.e5 (2021).
9. S. C. Moore, B. Kronsteiner, S. Longet, S. Adele, A. S. Deeks, C. Liu, W. Dejnirattisai, L. S. Reyes, N. Meardon, S. Faustini, S. Al-Taei, T. Tipton, L. M. Hering, A. Angyal, R. Brown, A. R. Nicols, S. L. Dobson, P. Supasa, A. Tuekprakhon, A. Cross, J. K. Tyerman, H. Hornsby, I. Grouneva, M. Plowright, P. Zhang, T. A. H. Newman, J. M. Nell, P. Abraham, M. Ali, T. Malone, I. Neale, E. Phillips, J. D. Wilson, A. Shields, E. C. Horner, L. H. Booth, L. Stafford, S. Bibi, D. G. Wootton, A. J. Mentzer, C. P. Conlon, K. Jeffery, P. C. Matthews, A. J. Pollard, A. Brown, S. L. Rowland-Jones, J. Mongkolsapaya, R. P. Payne, C. Dold, T. Lambe, J. E. D. Thaventhiran, G. Screaton, E. Barnes, S. Hopkins, V. Hall, C. J. Duncan, A. Richter, M. Carroll, T. I. de Silva, P. Klenerman, S. Dunachie; Lance Turtle PITCH Consortium, Evolution of long-term hybrid immunity in healthcare workers after different COVID-19 vaccination regimens: A longitudinal observational cohort study. medRxiv 2022.06.06.22275865 (2022). https://doi.org/10.1101/2022.06.06.22275865.
10. S. Crotty, Hybrid immunity. *Science* **372**, 1392–1393 (2021).
11. L. J. Abu-Raddad, H. Chemaitelly, H. H. Ayoub, S. AlMukdad, H. M. Yassine, H. A. Al-Khatib, M. K. Smatti, P. Tang, M. R. Hasan, P. Coyle, Z. Al-Kanaani, E. Al-Kuwari, A. Jeremijenko, A. H. Kaleeckal, A. N. Latif, R. M. Shaik, H. F. Abdul-Rahim, G. K. Nasrallah, M. G. Al-Kuwari, A. A. Butt, H. E. Al-Romaihi, M. H. Al-Thani, A. Al-Khal, R. Bertollini, Effect of mRNA vaccine boosters against SARS-CoV-2 Omicron infection in Qatar. *N. Engl. J. Med.* **386**, 1804–1816 (2022).
12. V. Hall, S. Foulkes, F. Insalata, P. Kirwan, A. Saei, A. Atti, E. Wellington, J. Khawam, K. Munro, M. Cole, C. Tranquillini, A. Taylor-Kerr, N. Hettiarachchi, D. Calbraith, N. Sajedi, I. Milligan, Y. Themistocleous, D. Corrigan, L. Cromey, L. Price, S. Stewart, E. de Lacy, C. Norman, E. Linley, A. D. Otter, A. Semper, J. Hewson, S. D'Arcangelo, M. Chand, C. S. Brown, T. Brooks, J. Islam, A. Charlett, S. Hopkins; F.R.C.P. for the SIREN Study Group, Protection against SARS-CoV-2 after Covid-19 vaccination and previous infection. *N. Engl. J. Med.* **386**, 1207–1220 (2022).
13. T. Cerqueira-Silva, J. R. Andrews, V. S. Boaventura, O. T. Ranzani, V. d. A. Oliveira, E. S. Paixão, J. B. Júnior, T. M. Machado, M. D. T. Hitchings, M. Dorion, M. L. Lind, G. O. Penna, D. A. T. Cummings, N. E. Dean, G. L. Werneck, N. Pearce, M. L. Barreto, A. I. Ko, J. Croda, M. Barral-Netto, Effectiveness of CoronaVac, ChAdOx1 nCoV-19, BNT162b2, and Ad26.COV2.S among individuals with previous SARS-CoV-2 infection in Brazil: A test-negative, case-control study. *Lancet Infect. Dis.* **22**, 791–801 (2022).
14. P. Nordström, M. Ballin, A. Nordström, Risk of SARS-CoV-2 reinfection and COVID-19 hospitalisation in individuals with natural and hybrid immunity: A retrospective, total population cohort study in Sweden. *Lancet Infect. Dis.* **22**, 781–790 (2022).
15. M. Bergwerk, T. Gonen, Y. Lustig, S. Amit, M. Lipsitch, C. Cohen, M. Mandelboim, E. Gal Levin, C. Rubin, V. Indenbaum, I. Tal, M. Zavitan, N. Zuckerman, A. Bar-Chaim, Y. Kreiss, G. Regev-Yochay, Covid-19 breakthrough infections in vaccinated health care workers. *N. Engl. J. Med.* **385**, 1474–1484 (2021).
16. Y. Araf, F. Akter, Y.-D. Tang, R. Fatemi, M. S. A. Parvez, C. Zheng, M. G. Hossain, Omicron variant of SARS-CoV-2: Genomics, transmissibility, and responses to current COVID-19 vaccines. *J. Med. Virol.* **94**, 1825–1832 (2022).
17. A. Sette, S. Crotty, Adaptive immunity to SARS-CoV-2 and COVID-19. *Cell* **184**, 861–880 (2021).
18. V. Legros, S. Denolly, M. Vogrig, B. Boson, J. Rigaill, S. Pillet, F. Grattard, S. Gonzalo, P. Verhoeven, O. Allatif, P. Berthelot, C. Pélissier, G. Thierry, E. Botelho-Nevers, S. Paul, T. Walzer, F.-L. Cosset, T. Bourlet, B. Pozzetto, A longitudinal study of SARS-CoV-2 infected patients shows high correlation between neutralizing antibodies and COVID-19 severity. *Cell Mol. Immunol.* **18**, 318–327 (2021).
19. H. Chemaitelly, P. Tang, M. R. Hasan, S. AlMukdad, H. M. Yassine, F. M. Benslimane, H. A. Al Khatib, P. Coyle, H. H. Ayoub, Z. Al Kanaani, E. Al Kuwari, A. Jeremijenko, A. H. Kaleeckal, A. N. Latif, R. M. Shaik, H. F. Abdul Rahim, G. K. Nasrallah, M. G. Al Kuwari, H. E. Al Romaihi, A. A. Butt, M. H. Al-Thani, A. Al Khal, R. Bertollini, L. J. Abu-Raddad, Waning of BNT162b2 vaccine protection against SARS-CoV-2 infection in Qatar. *N. Engl. J. Med.* **385**, e83 (2021).
20. E. G. Levin, Y. Lustig, C. Cohen, R. Fluss, V. Indenbaum, S. Amit, R. Doolman, K. Asraf, E. Mendelson, A. Ziv, C. Rubin, L. Freedman, Y. Kreiss, G. Regev-Yochay, Waning immune humoral response to BNT162b2 covid-19 vaccine over 6 months. *N. Engl. J. Med.* **385**, e84 (2021).
21. A. S. Breathnach, P. A. Riley, M. P. Cotter, A. C. Houston, M. S. Habibi, T. D. Planche, Prior COVID-19 significantly reduces the risk of subsequent infection, but reinfections are seen after eight months. *J. Infect.* **82**, e11–e12 (2021).
22. M. Peghin, E. Bouza, M. Fabris, M. De Martino, A. Palese, G. Bontempo, E. Graziano, V. Gerussi, V. Bressan, A. Sartor, M. Isola, C. Tascini, F. Curcio, Low risk of reinfections and relation with serological response after recovery from the first wave of COVID-19. *Eur. J. Clin. Microbiol. Infect. Dis.* **40**, 2597–2604 (2021).
23. S. Feng, D. J. Phillips, T. White, H. Sayal, P. K. Aley, S. Bibi, C. Dold, M. Fuskova, S. C. Gilbert, I. Hirsch, H. E. Humphries, B. Jepson, E. J. Kelly, E. Plested, K. Shoemaker, K. M. Thomas, J. Vekemans, T. L. Villafana, T. Lambe, A. J. Pollard, M. Voysey; Oxford COVID Vaccine Trial Group, Correlates of protection against symptomatic and asymptomatic SARS-CoV-2 infection. *Nat. Med.* **27**, 2032–2040 (2021).
24. P. B. Gilbert, D. C. Montefiori, A. B. McDermott, Y. Fong, D. Benkeser, W. Deng, H. Zhou, C. R. Houchens, K. Martins, L. Jayashankar, F. Castellino, B. Flach, B. C. Lin, S. O'Connell, C. McDanal, A. Eaton, M. Sarzotti-Kelsoe, Y. Lu, C. Yu, B. Borate, L. W. P. van der Laan, N. S. Hejazi, C. Huynh, J. Miller, H. M. El Sahly, L. R. Baden, M. Baron, L. De La Cruz, C. Gay, S. Kalams, C. F. Kelley, M. P. Andrasik, J. G. Kublin, L. Corey, K. M. Neuzil, L. N. Carpp, R. Pajon, D. Follmann, R. O. Donis, R. A. Koup; Immune Assays Team§; Moderna, Inc. Team§; Coronavirus Vaccine Prevention Network (CoVPN)/Coronavirus Efficacy (COVE) Team§; United States Government (USG)/CoVPN Biostatistics Team§, Immune correlates analysis of the mRNA-1273 COVID-19 vaccine efficacy clinical trial. *Science* **375**, 43–50 (2021).
25. EMA and ECDC recommendations on heterologous vaccination courses against COVID-19. *Eur. Cent. Dis. Prev. Control* (2021); https://ecdc.europa.eu/en/news-events/ema-and-ecdc-recommendations-heterologous-vaccination-courses-against-covid-19.
26. B. J. Gardner, A. M. Kilpatrick, Third doses of COVID-19 vaccines reduce infection and transmission of SARS-CoV-2 and could prevent future surges in some populations: A modeling study. medRxiv 2021.10.25.21265500 (2021). https://doi.org/10.1101/2021.10.25.21265500.
27. S. Terreri, E. P. Mortari, M. R. Vinci, C. Russo, C. Alteri, C. Albano, F. Colavita, G. Gramigna, C. Agrati, G. Linardos, L. Coltella, L. Colagrossi, G. Deriu, M. C. D. Atti, C. Rizzo, M. Scarsella, R. Brugaletta, V. Camisa, A. Santoro, G. Roscilli, E. Pavoni, A. Muzi, N. Magnavita, R. Scutari,

A. Villani, M. Raponi, F. Locatelli, C. F. Perno, S. Zaffina, R. Carsetti, Persistent B cell memory after SARS-CoV-2 vaccination is functional during breakthrough infections. *Cell Host Microbe* **30**, 400–408.e4 (2022).

28. M. Saadatian-Elahi, V. Picot, L. Hénaff, F. K. Pradel, V. Escuret, C. Dananché, C. Elias, H. P. Endtz, P. Vanhems, Protocol for a prospective, observational, hospital-based multicentre study of nosocomial SARS-CoV-2 transmission: NOSO-COR Project. *BMJ Open* **10**, e039088 (2020).
29. S. Trouillet-Assant, C. Albert Vega, A. Bal, J. A. Nazare, P. Fascia, A. Paul, A. Massardier-Pilonchery, C. d. Aubarede, N. Guibert, V. Pitiot, M. Lahousse, A. Boibieux, D. Makhloufi, C. Simon, M. Rabilloud, M. A. Trabaud, F. Gueyffier, J.-B. Fassier; COVID-SER study group, Assessment of serological techniques for screening patients for COVID-19 (COVID-SER): A prospective, multicentric study. *BMJ Open* **10**, e041268 (2020).
30. A. A. Mohan, L. B. Olson, I. A. Naqvi, S. A. Morrison, B. D. Kraft, L. Chen, L. G. Que, Q. Ma, C. E. Barkauskas, A. Kirk, S. K. Nair, B. A. Sullenger, G. Kasotakis, Age and comorbidities predict COVID-19 outcome, regardless of innate immune response severity: A single institutional cohort study. *Crit. Care Explor.* **4**, e0799 (2022).
31. C. Kaeuffer, C. L. Hyaric, T. Fabacher, J. Mootien, B. Dervieux, Y. Ruch, A. Hugerot, Y.-J. Zhu, V. Pointurier, R. Clere-Jehl, V. Greigert, L. Kassegne, N. Lefebvre, F. Gallais; Covid Alsace Study Group, N. Meyer, Y. Hansmann, O. Hinschberger, F. Danion; COVID Alsace Study Group, Clinical characteristics and risk factors associated with severe COVID-19: Prospective analysis of 1,045 hospitalised cases in North-Eastern France, March 2020. *Euro. Surveill.* **25**, 2000895 (2020).
32. C. Saade, C. Gonzalez, A. Bal, M. Valette, K. Saker, B. Lina, L. Josset, M.-A. Trabaud, G. Thiery, E. Botelho-Nevers, S. Paul, P. Verhoeven, T. Bourlet, S. Pillet, F. Morfin, S. Trouillet-Assant, B. Pozzetto; on behalf of COVID-SER study group, Live virus neutralization testing in convalescent patients and subjects vaccinated against 19A, 20B, 20I/501Y.V1 and 20H/501Y.V2 isolates of SARS-CoV-2. *Emerg. Microbes Infect.* **10**, 1499–1502 (2021).
33. W. Mouton, C. Compagnon, K. Saker, S. Daniel, S. Djebali, X. Lacoux, B. Pozzetto, G. Oriol, D. Laubreton, M. Prieux, J.-B. Fassier, N. Guibert, A. Massardier-Pilonchéry, D. Alfaiate, F. Berthier, T. Walzer, J. Marvel, K. Brengel-Pesce, S. Trouiller-Assant, Specific detection of memory T-cells in COVID-19 patients using standardized whole-blood Interferon gamma-release assay. *Eur. J. Immunol.* **51**, 3239–3242 (2021).
34. B. Pozzetto, V. Legros, S. Djebali, V. Barateau, N. Guibert, M. Villard, L. Peyrot, O. Allatif, J.-B. Fassier, A. Massardier-Pilonchéry, K. Brengel-Pesce, M. Yaugel-Novoa, S. Denolly, B. Boson, T. Bourlet, A. Bal, M. Valette, T. Andrieu, B. Lina; Covid-Ser study group, F.-L. Cosset, S. Paul, T. Defrance, J. Marvel, T. Walzer, S. Trouillet-Assant, Immunogenicity and efficacy of heterologous ChadOx1/BNT162b2 vaccination. *Nature* 600, 701–706 (2021).
35. X. Charmetant, M. Espi, I. Benotmane, V. Barateau, F. Heibel, F. Buron, G. Gautier-Vargas, M. Delafosse, P. Perrin, A. Koenig, N. Cognard, C. Levi, F. Gallais, L. Manière, P. Rossolillo, E. Soulier, F. Pierre, A. Ovize, E. Morelon, T. Defrance, S. Fafi-Kremer, S. Caillard, O. Thaunat, Infection or a third dose of mRNA vaccine elicits neutralizing antibody responses against SARS-CoV-2 in kidney transplant recipients. *Sci. Transl. Med.* **14**, eabl6141 (2022).
36. R. Morita, N. Schmitt, S.-E. Bentebibel, R. Ranganathan, L. Bourdery, G. Zurawski, E. Foucat, M. Dullaers, S. Oh, N. Sabzghabaei, E. M. Lavecchio, M. Punaro, V. Pascual, J. Banchereau, H. Ueno, Human Blood $CXCR5^+CD4^+$ T cells are counterparts of T follicular cells and contain specific subsets that differentially support antibody secretion. *Immunity* **34**, 108–121 (2011).
37. I. Sanz, C. Wei, S. A. Jenks, K. S. Cashman, C. Tipton, M. C. Woodruff, J. Hom, F. E.-H. Lee, Challenges and opportunities for consistent classification of human B cell and plasma cell populations. *Front. Immunol.* **10**, 2458 (2019).
38. S. A. Jenks, K. S. Cashman, E. Zumaquero, U. M. Marigorta, A. V. Patel, X. Wang, D. Tomar, M. C. Woodruff, Z. Simon, R. Bugrovsky, E. L. Blalock, C. D. Scharer, C. M. Tipton, C. Wei, S. S. Lim, M. Petri, T. B. Niewold, J. H. Anolik, G. Gibson, F. E.-H. Lee, J. M. Boss, F. E. Lund, I. Sanz, Distinct effector B cells induced by unregulated toll-like receptor 7 contribute to pathogenic responses in systemic lupus erythematosus. *Immunity* **49**, 725–739.e6 (2018).
39. S. A. Jenks, K. S. Cashman, M. C. Woodruff, F. E.-H. Lee, I. Sanz, Extrafollicular responses in humans and SLE. *Immunol. Rev.* **288**, 136–148 (2019).
40. E. L. Berg, T. Yoshino, L. S. Rott, M. K. Robinson, R. A. Warnock, T. K. Kishimoto, L. J. Picker, E. C. Butcher, The cutaneous lymphocyte antigen is a skin lymphocyte homing receptor for the vascular lectin endothelial cell-leukocyte adhesion molecule 1. *J. Exp. Med.* **174**, 1461–1466 (1991).
41. K. Hirahara, L. Liu, R. A. Clark, K. Yamanaka, R. C. Fuhlbrigge, T. S. Kupper, The majority of human peripheral blood $CD4^+CD25highFoxp3^+$ regulatory T cells bear functional skin-homing receptors. *J. Immunol.* **177**, 4488–4494 (2006).
42. M. van Splunter, E. van Hoffen, E. G. Floris-Vollenbroek, H. Timmerman, E. L. de Bos, B. Meijer, L. H. Ulfman, B. Witteman, J. M. Wells, S. Brugman, H. F. J. Savelkoul, R. J. J. van Neerven, Oral cholera vaccination promotes homing of IgA^+ memory B cells to the large intestine and the respiratory tract. *Mucosal Immunol.* **11**, 1254–1264 (2018).
43. L. M. Bradley, S. R. Watson, S. L. Swain, Entry of naive CD4 T cells into peripheral lymph nodes requires L-selectin. *J. Exp. Med.* **180**, 2401–2406 (1994).
44. J. V. Stein, A. Rot, Y. Luo, M. Narasimhaswamy, H. Nakano, M. D. Gunn, A. Matsuzawa, E. J. Quackenbush, M. E. Dorf, U. H. von Andrian, The Cc chemokine thymus-derived chemotactic agent 4 (Tca-4, secondary lymphoid tissue chemokine, 6ckine, exodus-2) triggers lymphocyte function–associated antigen 1–mediated arrest of rolling T lymphocytes in peripheral lymph node high endothelial venules. *J. Exp. Med.* **191**, 61–76 (2000).
45. W. E. Purtha, T. F. Tedder, S. Johnson, D. Bhattacharya, M. S. Diamond, Memory B cells, but not long-lived plasma cells, possess antigen specificities for viral escape mutants. *J. Exp. Med.* **208**, 2599–2606 (2011).
46. R. Kotaki, Y. Adachi, S. Moriyama, T. Onodera, S. Fukushi, T. Nagakura, K. Tonouchi, K. Terahara, L. Sun, T. Takano, A. Nishiyama, M. Shinkai, K. Oba, F. Nakamura-Uchiyama, H. Shimizu, T. Suzuki, T. Matsumura, M. Isogawa, Y. Takahashi, SARS-CoV-2 Omicron-neutralizing memory B cells are elicited by two doses of BNT162b2 mRNA vaccine. *Sci. Immunol.* **7**, eabn8590 (2022).
47. R. Harbecke, J. I. Cohen, M. N. Oxman, Herpes zoster vaccines. *J. Infect. Dis.* **224**, S429–S442 (2021).
48. K. Wild, M. Smits, S. Killmer, S. Strohmeier, C. Neumann-Haefelin, B. Bengsch, F. Krammer, M. Schwemmle, M. Hofmann, R. Thimme, K. Zoldan, T. Boettler, Pre-existing immunity and vaccine history determine hemagglutinin-specific CD4 T cell and IgG response following seasonal influenza vaccination. *Nat. Commun.* **12**, 6720 (2021).
49. I. Dogan, B. Bertocci, V. Vilmont, F. Delbos, J. Mégret, S. Storck, C.-A. Reynaud, J.-C. Weill, Multiple layers of B cell memory with different effector functions. *Nat. Immunol.* **10**, 1292–1299 (2009).
50. K. A. Pape, J. J. Taylor, R. W. Maul, P. J. Gearhart, M. K. Jenkins, Different B cell populations mediate early and late memory during an endogenous immune response. *Science* **331**, 1203–1207 (2011).
51. G. V. Zuccarino-Catania, S. Sadanand, F. J. Weisel, M. M. Tomayko, H. Meng, S. H. Kleinstein, K. L. Good-Jacobson, M. J. Shlomchik, CD80 and PD-L2 define functionally distinct memory B cell subsets that are independent of antibody isotype. *Nat. Immunol.* **15**, 631–637 (2014).
52. A. Sokal, G. Barba-Spaeth, I. Fernández, M. Broketa, I. Azzaoui, A. de La Selle, A. Vandenberghe, S. Fourati, A. Roeser, A. Meola, M. Bouvier-Alias, E. Crickx, L. Languille, M. Michel, B. Godeau, S. Gallien, G. Melica, Y. Nguyen, V. Zarrouk, F. Canoui-Poitrine, F. Pirenne, J. Mégret, J.-M. Pawlotsky, S. Fillatreau, P. Bruhns, F. A. Rey, J.-C. Weill, C.-A. Reynaud, P. Chappert, M. Mahévas, mRNA vaccination of naive and COVID-19-recovered individuals elicits potent memory B cells that recognize SARS-CoV-2 variants. *Immunity* **54**, 2893–2907.e5 (2021).
53. L. B. Rodda, P. A. Morawski, K. B. Pruner, M. L. Fahning, C. A. Howard, N. Franko, J. Logue, J. Eggenberger, C. Stokes, I. Golez, M. Hale, M. Gale, H. Y. Chu, D. J. Campbell, M. Pepper, Imprinted SARS-CoV-2-specific memory lymphocytes define hybrid immunity. *Cell* **185**, 1588–1601.e14 (2022).
54. S. L. Stone, J. N. Peel, C. D. Scharer, C. A. Risley, D. A. Chisolm, M. D. Schultz, B. Yu, A. Ballesteros-Tato, W. Wojciechowski, B. Mousseau, R. S. Misra, A. Hanidu, H. Jiang, Z. Qi, J. M. Boss, T. D. Randall, S. R. Brodeur, A. W. Goldrath, A. S. Weinmann, A. F. Rosenberg, F. E. Lund, T-bet transcription factor promotes antibody-secreting cell differentiation by limiting the inflammatory effects of IFN-γ on B cells. *Immunity* **50**, 1172–1187.e7 (2019).
55. E. Zumaquero, S. L. Stone, C. D. Scharer, S. A. Jenks, A. Nellore, B. Mousseau, A. Rosal-Vela, D. Botta, J. E. Bradley, W. Wojciechowski, T. Ptacek, M. I. Danila, J. C. Edberg, S. L. Bridges Jr., R. P. Kimberly, W. W. Chatham, T. R. Schoeb, A. F. Rosenberg, J. M. Boss, I. Sanz, F. E. Lund, IFNγ induces epigenetic programming of human T-bethi B cells and promotes TLR7/8 and IL-21 induced differentiation. *eLife* **8**, e41641 (2019).
56. N. Kaneko, H.-H. Kuo, J. Boucau, J. R. Farmer, H. Allard-Chamard, V. S. Mahajan, A. Piechocka-Trocha, K. Lefteri, M. Osborn, J. Bals, Y. C. Bartsch, N. Bonheur, T. M. Caradonna, J. Chevalier, F. Chowdhury, T. J. Diefenbach, K. Einkauf, J. Fallon, J. Feldman, K. K. Finn, P. Garcia-Broncano, C. A. Hartana, B. M. Hauser, C. Jiang, P. Kaplonek, M. Karpell, E. C. Koscher, X. Lian, H. Liu, J. Liu, N. L. Ly, A. R. Michell, Y. Rassadkina, K. Seiger, L. Sessa, S. Shin, N. Singh, W. Sun, X. Sun, H. J. Ticheli, M. T. Waring, A. L. Zhu, G. Alter, J. Z. Li, D. Lingwood, A. G. Schmidt, M. Lichterfeld, B. D. Walker, X. G. Yu, R. F. Padera, S. Pillai; Massachusetts Consortium on Pathogen Readiness Specimen Working Group, Loss of Bcl-6-expressing T follicular helper cells and germinal centers in COVID-19. *Cell* **183**, 143–157.e13 (2020).
57. A. Sokal, P. Chappert, G. Barba-Spaeth, A. Roeser, S. Fourati, I. Azzaoui, A. Vandenberghe, I. Fernandez, A. Meola, M. Bouvier-Alias, E. Crickx, A. Beldi-Ferchiou, S. Hue, L. Languille, M. Michel, S. Baloul, F. Noizat-Pirenne, M. Luka, J. Mégret, M. Ménager, J.-M. Pawlotsky, S. Fillatreau, F. A. Rey, J.-C. Weill, C.-A. Reynaud, M. Mahévas, Maturation and persistence of the anti-SARS-CoV-2 memory B cell response. *Cell* **184**, 1201–1213.e14 (2021).
58. S. R. Allie, J. E. Bradley, U. Mudunuru, M. D. Schultz, B. A. Graf, F. E. Lund, T. D. Randall, The establishment of resident memory B cells in the lung requires local antigen encounter. *Nat. Immunol.* **20**, 97–108 (2019).
59. C. M. Tipton, C. F. Fucile, J. Darce, A. Chida, T. Ichikawa, I. Gregoretti, S. Schieferl, J. Hom, S. Jenks, R. J. Feldman, R. Mehr, C. Wei, F. E.-H. Lee, W. C. Cheung, A. F. Rosenberg, I. Sanz,

Diversity, cellular origin and autoreactivity of antibody-secreting cell population expansions in acute systemic lupus erythematosus. *Nat. Immunol.* **16**, 755–765 (2015).
60. R. Keating, T. Hertz, M. Wehenkel, T. L. Harris, B. A. Edwards, J. L. McClaren, S. A. Brown, S. Surman, Z. S. Wilson, P. Bradley, J. Hurwitz, H. Chi, P. C. Doherty, P. G. Thomas, M. A. McGargill, The kinase mTOR modulates the antibody response to provide cross-protective immunity to lethal infection with influenza virus. *Nat. Immunol.* **14**, 1266–1276 (2013).
61. Y. Chen, P. Tong, N. Whiteman, A. S. Moghaddam, M. Zarghami, A. Zuiani, S. Habibi, A. Gautam, F. Keerti, C. Bi, T. Xiao, Y. Cai, B. Chen, D. Neuberg, D. R. Wesemann, Immune recall improves antibody durability and breadth to SARS-CoV-2 variants. *Sci. Immunol.* **7**, eabp8328 (2022).
62. F. D'Amico, S. Danese, L. Peyrin-Biroulet, Systematic review on inflammatory bowel disease patients with coronavirus disease 2019: It is time to take stock. *Clin. Gastroenterol. Hepatol.* **18**, 2689–2700 (2020).
63. J. V. Patankar, M. T. Chiriac, M. Lehmann, A. A. Kühl, R. Atreya, C. Becker, M. G.-A. Callaborators, H. Schmitt, R. Gamez-Belmonte, M. Mahapatro, L. Diemand, L. Hartmann, F. Mascia, Z. Hracsko, V. Thonn, L. Schödel, M. Zielinska, Y. Yu, L. Erkert, W. Li, M. Zeitler, B. Ruder, I. Ganzleben, C. Günther, D. Voehringer, S. Zundler, M. F. Neurath, B. Siegmund, Severe acute respiratory syndrome coronavirus 2 attachment receptor angiotensin-converting enzyme 2 is decreased in Crohn's disease and regulated by microbial and inflammatory signaling. *Gastroenterology* **160**, 925–928.e4 (2021).
64. T. M. Müller, E. Becker, M. Wiendl, L. L. Schulze, C. Voskens, S. Völkl, A. E. Kremer, M. F. Neurath, S. Zundler, Circulating adaptive immune cells expressing the gut homing marker α4β7 integrin are decreased in COVID-19. *Front. Immunol.* **12**, 639329 (2021).
65. P. Sundström, S. B. Lundin, L.-A. Nilsson, M. Quiding-Järbrink, Human IgA-secreting cells induced by intestinal, but not systemic, immunization respond to CCL25 (TECK) and CCL28 (MEC). *Eur. J. Immunol.* **38**, 3327–3338 (2008).
66. L. Azzi, D. D. Gasperina, G. Veronesi, M. Shallak, G. Ietto, D. Iovino, A. Baj, F. Gianfagna, V. Maurino, D. Focosi, F. Maggi, M. M. Ferrario, F. Dentali, G. Carcano, A. Tagliabue, L. S. Maffioli, R. S. Accolla, G. Forlani, Mucosal immune response in BNT162b2 COVID-19 vaccine recipients. *eBioMedicine* **75**, 103788 (2022).
67. F. Qadri, P. H. Mäkelä, J. Holmgren, M. J. Albert, K. Mannoor, A. Kantele, D. Saha, M. A. Salam, J. M. Kantele, Enteric infections in an endemic area induce a circulating antibody-secreting cell response with homing potentials to both mucosal and systemic tissues. *J. Infect. Dis.* **177**, 1594–1599 (1998).
68. M. Quiding-Järbrink, I. Nordström, G. Granström, A. Kilander, M. Jertborn, E. C. Butcher, A. I. Lazarovits, J. Holmgren, C. Czerkinsky, Differential expression of tissue-specific adhesion molecules on human circulating antibody-forming cells after systemic, enteric, and nasal immunizations. A molecular basis for the compartmentalization of effector B cell responses. *J. Clin. Invest.* **99**, 1281–1286 (1997).
69. F. Ntziora, E. G. Kostaki, A. Karapanou, M. Mylona, I. Tseti, N. V. Sipsas, D. Paraskevis, P. P. Sfikakis, Protection of vaccination versus hybrid immunity against infection with COVID-19 Omicron variants among health care workers. *Vaccine* **40**, 7195–7200 (2022).
70. A. Bal, B. Pozzetto, M.-A. Trabaud, V. Escuret, M. Rabilloud, C. Langlois-Jacques, A. Paul, N. Guibert, C. D'Aubarède-Frieh, A. Massardier-Pilonchery, N. Fabien, D. Goncalves, A. Boibieux, F. Morfin-Sherpa, V. Pitiot, F. Gueyffier, B. Lina, J.-B. Fassier, S. Trouillet-Assant; COVID SER Study Group, Evaluation of high-throughput SARS-CoV-2 serological assays in a longitudinal cohort of patients with mild COVID-19: Clinical sensitivity, specificity, and association with virus neutralization test. *Clin. Chem.* **67**, 742–752 (2021).
71. F. Amanat, D. Stadlbauer, S. Strohmeier, T. H. O. Nguyen, V. Chromikova, M. McMahon, K. Jiang, G. A. Arunkumar, D. Jurczyszak, J. Polanco, M. Bermudez-Gonzalez, G. Kleiner, T. Aydillo, L. Miorin, D. S. Fierer, L. A. Lugo, E. M. Kojic, J. Stoever, S. T. H. Liu, C. Cunningham-Rundles, P. L. Felgner, T. Moran, A. García-Sastre, D. Caplivski, A. C. Cheng, K. Kedzierska, O. Vapalahti, J. M. Hepojoki, V. Simon, F. Krammer, A serological assay to detect SARS-CoV-2 seroconversion in humans. *Nat. Med.* **26**, 1033–1036 (2020).
72. A. Pizzorno, B. Padey, T. Julien, S. Trouillet-Assant, A. Traversier, E. Errazuriz-Cerda, J. Fouret, J. Dubois, A. Gaymard, F.-X. Lescure, V. Dulière, P. Brun, S. Constant, J. Poissy, B. Lina, Y. Yazdanpanah, O. Terrier, M. Rosa-Calatrava, Characterization and treatment of SARS-CoV-2 in nasal and bronchial human airway epithelia. *Cell Rep. Med.* **1**, 100059 (2020).
73. E. D. Amir, K. L. Davis, M. D. Tadmor, E. F. Simonds, J. H. Levine, S. C. Bendall, D. K. Shenfeld, S. Krishnaswamy, G. P. Nolan, D. Pe'er, viSNE enables visualization of high dimensional single-cell data and reveals phenotypic heterogeneity of leukemia. *Nat. Biotechnol.* **31**, 545–552 (2013).

Acknowledgments: We acknowledge the contribution of SFR Biosciences (UAR3444/CNRS, US8/Inserm, ENS de Lyon, UCBL), AniRA-cytometry, E. Devêvre, and S. Dussurgey. We thank the following staff members and individuals: all the staff members of the Occupational Health and Medicine Department of the Hospices Civils de Lyon and staff members who contributed to the IMMUNO-NOSOCOR clinical study (who contributed to the sample collection), all the clinical research associates for excellent work, and all the members of the clinical research and innovation department for reactivity (DRCI, Hospices Civils de Lyon). Special thanks to members of the Lyon-COVID study group for participation in patient recruitment and technical optimization: K. Saker, B. Mokdad, C. d'Aubarede, V. Pitiot, A. Bal, F. Morfin, M. Trabaud, M. Prieux, V. Dubois, L. Josset, S. Daniel, F. Berthier, S. Bennia, C. Mena, C. Planckaert, N. Trehet-Mandez, N. Paquin, R. Chapurlat, A. Termoz, J. Haesebaert, B. Leveau, V. Icard, V. Escuret, J. Cussey, A. Metzinger, C. Guyard, C. Mignon, C. Hesslinger, Y. Ataman-Onal, C. Henquell, B. Souweine, H. Pelloux, T. Bourlet, F. Venet, and N. Bomchil. Last, we thank all the patients and the health care workers for participation in this clinical study. Human biological samples and associated data were obtained from NeuroBioTec (CRB HCL, Lyon France, Biobank BB-0033-00046). **Funding:** This study was supported by grants from ANRS-MIE (Emergen study, grant ANRS-0154 attributed to B.L.), REACTing (Research and ACTion targeting emerging infectious diseases, attributed to T.W.), the AnBer Foundation (attributed to P.V.), the COVID AURA translate consortium (FEDER/FSE Rhône-Alpes, FINOVI foundation, and BULLUKIAN foundation, attributed to J.C.), and institutional grants from INSERM, CNRS, UCBL1, and ENS de Lyon. These different funding sources had no role in study design, collection, analysis, interpretation of data, writing of the report, or the decision to submit the paper for publication. **Author contributions:** V.B. and L.P. conducted the phenotypical analysis of RBD-specific mBCs. C.S. and B.P. conducted assessment of serological B cell memory and virus neutralization assays. D.M.-B., M.-H.E., and O.A. performed all statistical analyses. N.G. took care of patient recruitment. N.M. and J.C. conducted experiments measuring RBD-specific IgG avidity. K.B.-P., C.C., and S.D. realized the IFN-γ release assays. J.-B.F. analyzed the clinical infection data. K.L. and M.E. contributed to the phenotypical analysis of spike protein–specific $CD4^+$ T cells. B.L., M.R.-C., J.M., and O.T. supervised the experimental tasks. A.P. performed and analyzed data related to viral infection in reconstituted HAE. P.V., L.H., and M.S.-E. participated in the Immunonosocor study, including patient recruitment and database development. T.D., S.P., T.W., and S.T.-A. designed the study, analyzed the data, and wrote the manuscript. **Competing interests:** K.B.-P. and C.C. are Biomérieux employees. O.T. has received consulting fees from AstraZeneca related to COVID-19. The other authors declare that they have no competing interests. **Data and materials availability:** All data associated with this study are present in the paper or the Supplementary Materials. Requests for data should be addressed to the corresponding authors.

Submitted 21 July 2022
Accepted 9 February 2023
Published 15 March 2023
10.1126/scitranslmed.ade0550

Science Translational Medicine

Prior SARS-CoV-2 infection enhances and reshapes spike protein–specific memory induced by vaccination

Vronique Barateau, Loc Peyrot, Carla Saade, Bruno Pozzetto, Karen Brengel-Pesce, Mad-Hlnie Elsensohn, Omran Allatif, Nicolas Guibert, Christelle Compagnon, Natacha Mariano, Julie Chaix, Sophia Djebali, Jean-Baptiste Fassier, Bruno Lina, Katia Lefsihane, Maxime Espi, Olivier Thaunat, Jacqueline Marvel, Manuel Rosa-Calatrava, Andres Pizzorno, Delphine Maucort-Boulch, Laetitia Henaff, Mitra Saadatian-Elahi, Philippe Vanhems, Stphane Paul, Thierry Walzer, Sophie Trouillet-Assant, and Thierry Defrance

Sci. Transl. Med., **15** (687), eade0550.
DOI: 10.1126/scitranslmed.ade0550